OCEANICS
INC.

AD614672

EXPERIMENTAL MODEL STUDIES OF THE DYNAMIC VELOCITY

FLUCTUATIONS EXISTING IN THE AIR WAKE

OF AN AIRCRAFT CARRIER

Part I: TEXT

by

August F. Lehman

and

Paul Kaplan

Report No. 65-21
Part I

March, 1965

Technical Industrial Park / Plainview, N.Y.

EXPERIMENTAL MODEL STUDIES OF THE DYNAMIC VELOCITY

FLUCTUATIONS EXISTING IN THE AIR WAKE

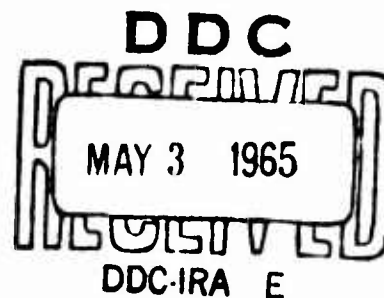OF AN AIRCRAFT CARRIER

Part I: TEXT

by

August F. Lehman

and

Paul Kaplan

Report No. 65-21   March, 1965
Part I

¯OCEANICS¯

ABSTRACT

Experimental investigations were undertaken in a water tunnel to measure the dynamic horizontal and vertical velocity fluctuations existing in the air wake of a carrier and encountered by landing aircraft.

A description of the instrumentation developed, and an analysis of the methods employed in converting data to pitch transfer functions (amplitude and phase) is given together with the determination of power spectra information.

Conclusions regarding instrumentation, test data interpretation and operational procedures for the carrier and aircraft are presented.

i

OCEANICS

TABLE OF CONTENTS

OCEANICS

OCEANICS

LIST OF ILLUSTRATIONS

Page No.

iv

v

OCEANICS

APPENDIX MATERIAL

OCEANICS

NOMENCLATURE

—OCEANICS—

L   =   length

p   =   pressure

t   =   time

U   =   free stream velocity (wind-over-deck speed)

U_a =   average axial velocity

u   =   fluctuating component of axial velocity

W_a =   average vertical velocity

w   =   fluctuating component of vertical velocity

x   =   axial coordinate

z   =   vertical coordinate

θ   =   pitch angle (radians)

μ   =   dynamic viscosity

ρ   =   mass density

$\overline{\Phi}$ =   power spectral density

ψ   =   angle of oncoming wind with respect to ship centerline

ω   =   circular frequency (rad./sec.)

—OCEANICS—

ACKNOWLEDGEMENTS

OCEANICS

INTRODUCTION

The processes involved in landing an aircraft on a carrier while the ship is undergoing pitching, heaving and rolling motions are rather complex. The risk hazard is high and the penalty can be severe for a miscalculation on the part of the pilot. To aid the pilot in the execution of a successful approach and landing, a landing signal system such as the Fresnel Lens Optical Landing System is used. With this system or with any similar signal system, there are three major elements involved; viz.

1- ship dynamics,

2- aircraft dynamics, and

3- pilot response.

The programming of the above parameters in simulator studies, including the variation of these parameters up to their expected limits, is one method which can be used to identify areas where the highest "pay-off" exists in terms of improvement of overall system performance. Studies of this nature have been and are being undertaken by Systems Technology, Inc., of Hawthorne, California [1].

One of the environmental conditions which requires more detailed study, as indicated by investigations undertaken by Systems Technology, Inc., was the nature of the

"turbulence"* existing in the wake of a carrier. Turbulence is recognized as being of major concern by carrier based pilots and one facet of disturbed flow is commonly referred to as a "burble".

Visualization studies of the dynamic air wake undertaken by Oceanics [2] provided visual proof of the existence of this burble. In addition to the visualization studies devoted to the air wake existing with carrier motions, studies of the wake associated with a stationary (no pitch, heave or roll) model also provided information on the "steady" velocity magnitudes and directions existing in the wake for a considerable distance downstream.

PROGRAM OBJECTIVES

In order to obtain data on the time-dependent velocity disturbances existing in the wake, the following objectives were established:

1- to undertake water tunnel tests permitting the measurement and evaluation of dynamic velocity fluctuations (in both the axial and vertical directions) in the flow field surrounding the normal glide path employed

---

*Identified here as large macroscopic disturbances in the fluid flow field.

by aircraft in the process of landing on an
aircraft carrier, and

2- to analyze and interpret the data so as to permit
its utilization in simulator studies concerned with
the Fresnel Lens Optical Landing System.

In satisfying these objectives, and as specified in
the contractual task assignment, Oceanics, Inc. maintained close
liaison and exchange of data with Systems Technology, Inc. where
Systems Technology's task (under Contract No. Nonr-4156(00))
employed the "air" wake model input data from Oceanics in the
overall systems analysis of the carrier landing problem.

General Approach to the Problem

As pointed out in [2], the use of a water tunnel for
air wake studies is quite reasonable. At full scale wind-over-
deck velocities, air acts as an incompressible fluid, i.e. the
compressibility effects are negligible. Because the air acts as
an incompressible fluid, water, which is an incompressible fluid,
can be satisfactorily substituted. (Conversely, problems in-
volving water flow can be, and often are, studied in low velocity
air flows.) Thus, water tunnel studies are as valid as air
tunnel studies. In fact, from Reynolds number* scaling

---

*A dimensionless parameter used in fluid mechanics studies where
the controlling variables in a problem are considered to be
velocity, length, mass density and dynamic viscosity.

considerations, water tunnel studies have a decided advantage over air tunnel studies because of the difference in the kinematic viscosity of the two fluids. The wall effects in water tunnel studies are no larger than those in air tunnel studies. Boundary layer growth has a direct relationship with Reynolds number, thus the same boundary layer exists in either an air or a water tunnel if the tests are run at the same Reynolds number. For the size of model and test section employed here, wall effects are considered negligible. This was established in [2].

The model had an overall length of 33 inches. This model size, together with the tunnel test section length of 7 feet, permitted downstream measurements which adequately covered areas wherein the burble disturbance is normally encountered. According to information from Systems Technology, as well as conversations with carrier based pilots, the disturbances in the glide path are of serious concern in the last several seconds before touchdown. With an aircraft closure rate of approximately 100 knots, the disturbances thus normally lie within 700-800 feet aft of touchdown.

In the flow visualization studies [2], tests were made with and without the island on the model. However, it was quite apparent from those studies that the island contributes little to the disturbed flow pattern when carrier motions exist. For that reason, the current studies did not include observations without the island.

Oceanics Water Tunnel

The Oceanics water tunnel is a closed jet, recirculating type of tunnel having both the velocity and pressure variable. The maximum test section velocity is about 40 feet per second, while the test section pressure, which can be controlled independently of the test section velocity, covers a range from about -0.9 atmospheres to +1.0 atmospheres using atmospheric reference. The test section itself is about 20 inches on a side, having rounded corners. The overall length of the test section is 7 feet, as mentioned earlier. There are eight viewing windows; two on each of the four sides, with each window having a viewing area of 10x30 inches.

Test Arrangement

The test arrangement for this phase of the program was also the same as that successfully employed in earlier phases. Essentially it consisted of having a flat horizontal plate extending across the width and length of the test section. This plate thus represented the sea surface and divided the flow passing through the test section. The flow of water passing over the upper portion of the plate represents air flow in the real case. This is the portion of the flow which is of interest in this program. (The flow below the plate has no significance in this study.)

The model was positioned near the forward end of the test section and the null actually passed through an opening in the plate. This opening was just large enough to permit the model to undergo heaving, pitching and rolling motions without hitting the sides of the opening. The model was actually supported by rods extending from the pitch and heave actuation mechanism (located beneath the test section) through the tunnel floor and into the model mounting block. Roll actuation is controlled by a separate push-pull mechanism. Figure 1 is a sketch of the basic model-plate-actuation installation.

Measurements of the dynamic velocity fluctuations (in both the axial and vertical directions) were taken at various "windows" along the glide path using a dynamic sensing pressure probe designed and developed as a part of this program. Figure 2 is a sketch, while Figures 3 and 4 are photographs, illustrating this installation.

The initial intent of the program was to undertake measurements in the air wake only with motions of the model, but the program scope was later modified at the suggestion of Systems Technology, Inc., (with the approval of the ONR Project Officer) to include certain specific measurements (power spectra) of the wake without motions of the model. As pitch motions apparently caused the greatest disturbances in

MODEL MOUNTING BLOCK

FAIRING

TUNNEL FLOOR

SUPPORT (AND ACTUATION) RODS

PITCH AND HEAVE
ACTUATION MECHANISM

FALSE FLOOR SIMULATING
SEA SURFACE

ROLL ACTUATION CABLE
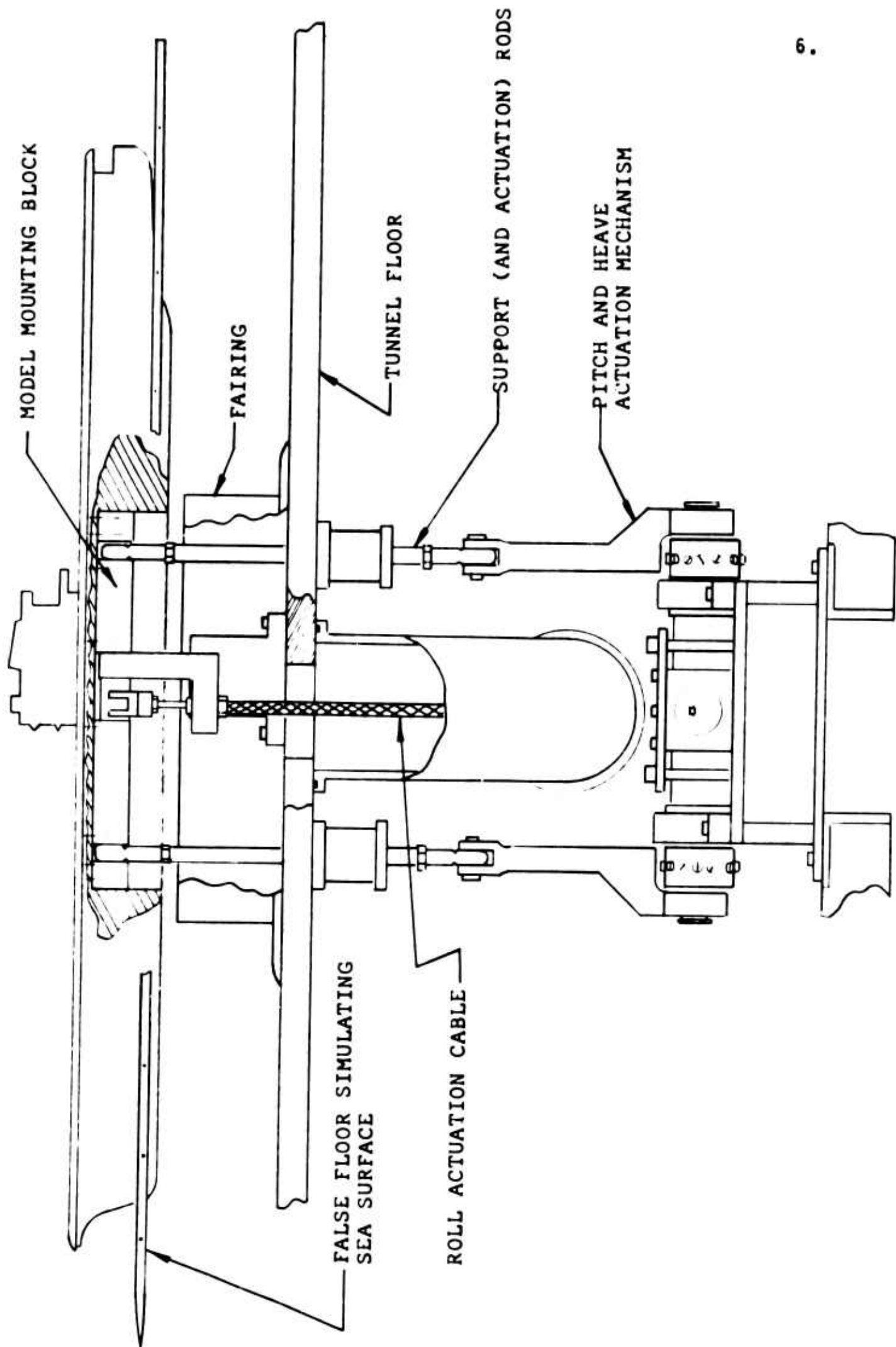
FIGURE 1   SKETCH OF TUNNEL INSTALLATION

OCEANICS

MEASURING PLANES
(EQUIVALENT FULL SCALE DISTANCES)

1040'

764'

485'

226'

FLOW

OCEANICS
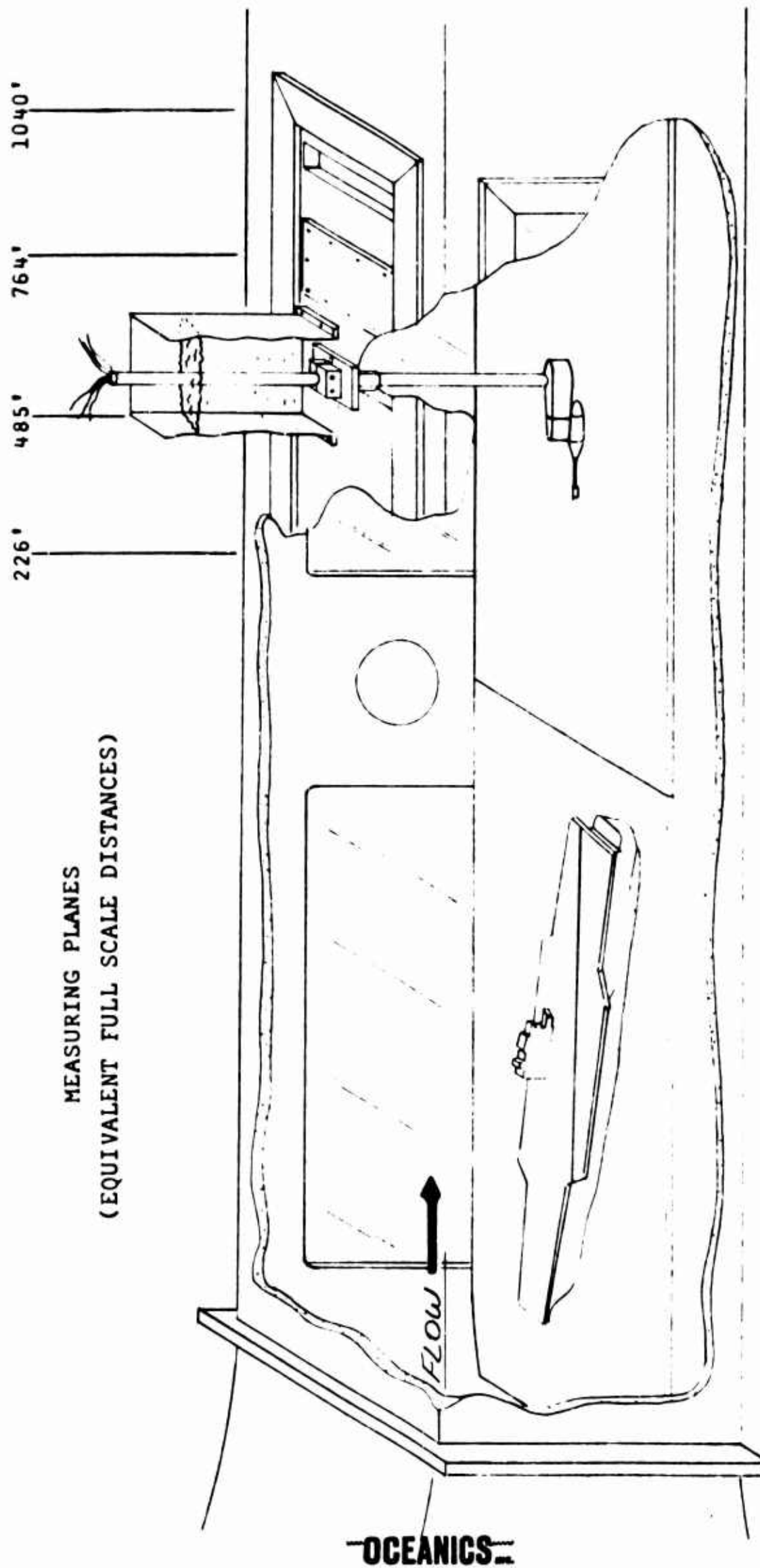
FIGURE 2   SKETCH OF GENERAL TEST ARRANGEMENT
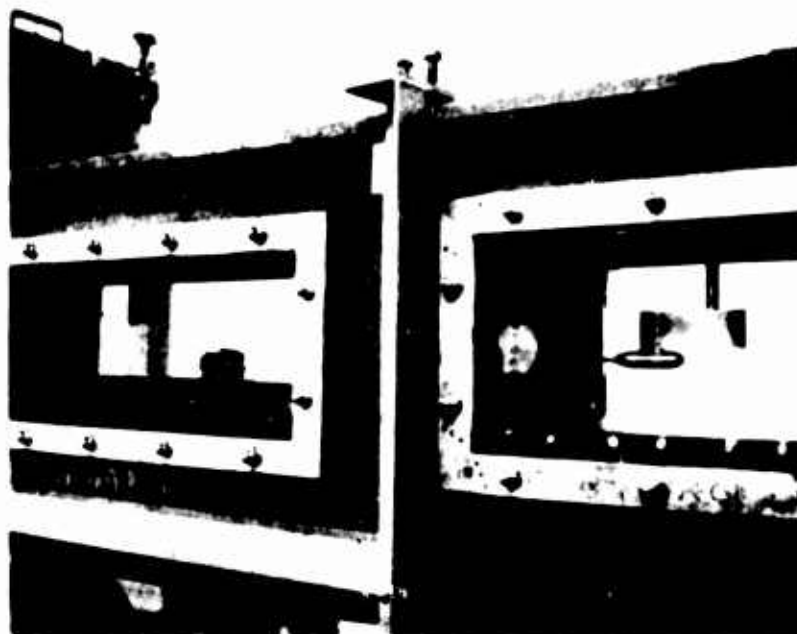
FIGURE 3 TYPICAL TUNNEL INSTALLATION OF PROBE USED FOR
AXIAL MEASUREMENTS
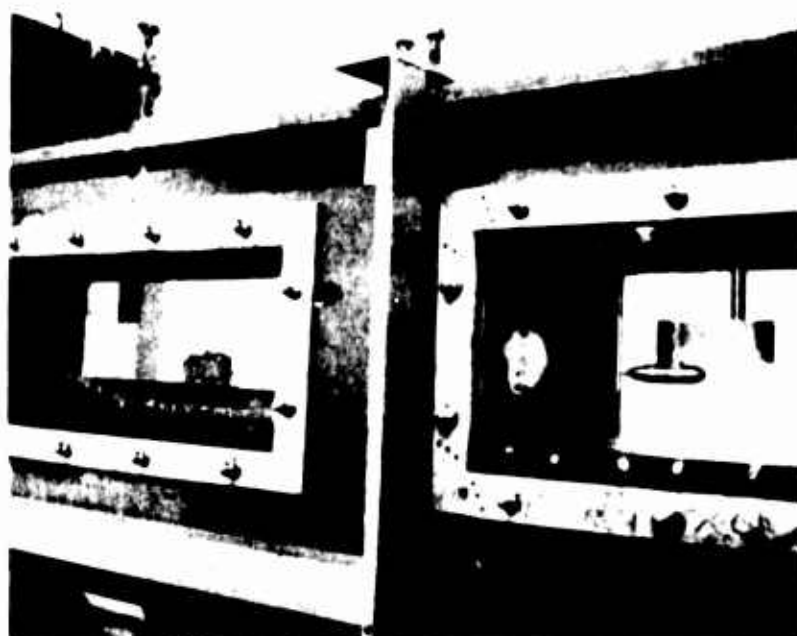
FIGURE 4 TYPICAL TUNNEL INSTALLATION OF PROBE USED FOR
TRANSVERSE MEASUREMENTS

the dynamic wake, studies with carrier motion were confined
to those involving pitch [2].

DYNAMIC VELOCITY MEASUREMENT TECHNIQUE

The key to the success of this phase of the program
lay in the development of a sensing probe which would satis-
factorily detect the unsteady axial and vertical velocity
components in a liquid flow field. There are three major
elements comprising the overall system:

1- the probe or sensing element,

2- the method of calibrating the probe, and

3- the recording of the probe's signal such that phase
   relationships can be made at specific frequencies
   of interest.

Probe or Sensing Element

The development of a successful unsteady velocity
sensing element has received considerable attention in the
past decade or so. Hubbard and Ling [3] developed a hot
film probe closely patterned after the well-known hot wire
technique successfully employed for turbulence measurements
in air tunnels. The Hubbard-Ling probe has been used with
some success by a few investigators, but for the most part
remains rather tempermental (although perhaps not significantly

more than some hot wire devices developed for use in air).
The development of a thermistor probe has been pushed rather
extensively during the last 4 or 5 years at the Ordnance
Research Laboratory under the guidance of Dr. John Lumley*
and offers considerable promise, but at the time of under-
taking these investigations Dr. Lumley did not believe it
had been developed sufficiently to serve as the type of
rugged instrument desired for these investigations. What was
wanted here was an extremely rugged instrument, holding its
calibration for several weeks (if not months) and having no
tempermental characteristics when subjected to the environment
of a "typical" water tunnel. In short, what was de ired was
an instrument approaching the reliability and simplicity of
a standard Prandtl type pitot tube.

For this particular investigation, a significant
advantage existed in that the desired frequency response
range is exceptionally low when compared with the response
range desired by typical turbulence detection devices. For
example, the maximum full scale ω range with pitch motions
was in the neighborhood of unity; thus in our model scale
the maximum frequency was about 10 cycles per second. For
power spectra, the desired maximum full scale ω value was of
the order of three, corresponding to a model scale frequency

*Professor of Aeronautical Engineering, Pennsylvania State Univ.

of the order of 30 cycles per second.

Because of the low frequency requirements, it was our belief that a probe utilizing small commercially available pressure transducers (Consolidated Electrodynamics Corporation, type 4-312-002) could be used. Basically, the concept involved a Prandtl-type pitot tube extending from a streamlined pod, this pod containing the pressure transducers. A sketch of the probe is shown in Figure 5. Here it can be noted that the total head pressure is fed to one transducer, with the static head pressure fed to the other. The electrical output from the transducers is subtracted, one from the other, leaving a signal which is some measure of the velocity head.

In a sense, this instrument has much in common with that developed by the Department of Civil and Sanitary Engineering at Massachusetts Institute of Technology. The device developed there consisted of a total head impact tube terminating in a specially constructed pressure transducer. That instrument and the test results obtained with it in certain free surface flow investigations are well presented in [4]. The advantages of the present probe are that it is considerably smaller, the transducers are commercially available, and that both the total (or impact) pressure and the static pressure are sensed by the instrument.

ELECTRICAL LEADS FROM TRANSDUCERS

CEC TRANSDUCER

CEC TRANSDUCER

EPOXY

TOTAL HEAD PRESSURE

STATIC HEAD PRESSURE

2X SIZE

1.812

3 D SKETCH OF SHIELD FOR AXIAL MEASUREMENTS
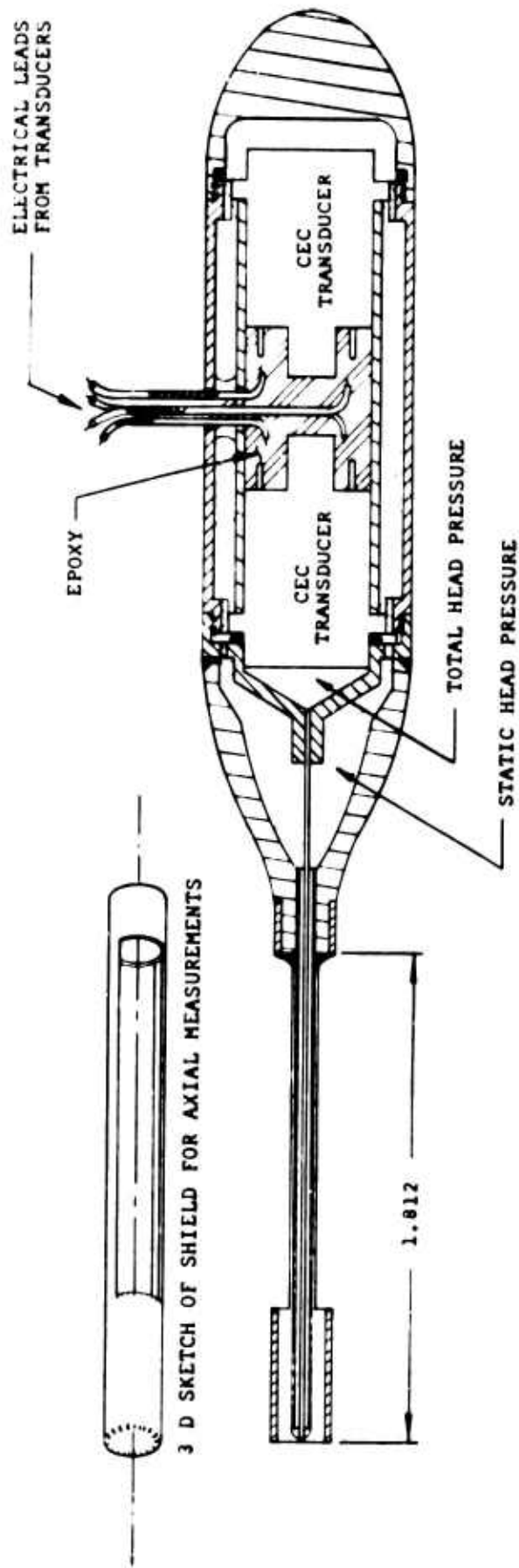
0.059 O.D.; 0.009 WALL; 17 GAGE STAINLESS TUBING

0.025 O.D.; 0.0062 WALL; 23 GAGE STAINLESS TUBING

3 STATIC PRESSURE OPENINGS 0.031 DIA. EQUALLY SPACED

.100

0.200

0.250

.500
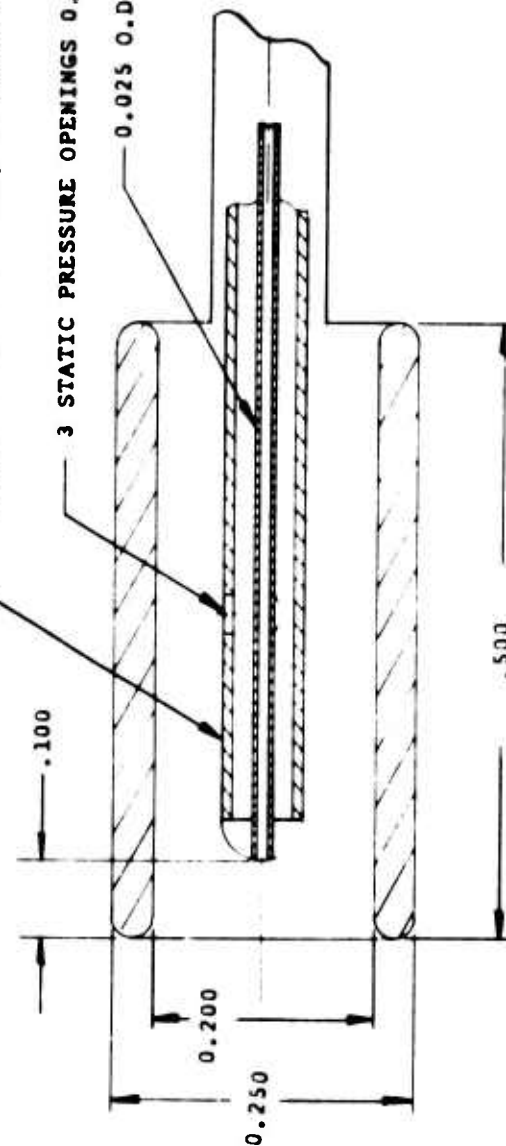
8X DETAILS OF AXIAL PROBE TIP AND SHIELD

.156

.100

.625

2X DETAIL OF VERTICAL PROBE TIP AND SHIELD SAME AS AXIAL EXCEPT FOR 90° BEND

ALL DIMENSIONS ARE IN INCHES

FIGURE 5   SKETCH OF PROBE

OCEANICS

12.

The transducers themselves have a natural frequency
of 3000 cycles per second in air. This is several orders of
magnitude higher than the upper limit of frequencies desired
to be investigated in this program. There is, of course, some
damping in the response of the probe due to additional fluid
mass effects and to fluid transport in the system occurring
when the face of the transducer deflects as a result of a
change in pressure. However, the deflections of the transducer
face are extremely minute, thus the amount of water transport
should be quite small.

The size of the tip or sensing portion of this
probe, while not as small as a hot wire, is considered
sufficiently small for the frequency range of interest. Also,
the energy in disturbed water is contained in a much lower
frequency range than that associated with air flows. For
example, from [4] it is stated that "...for the flows investi-
gated, 50% of the turbulent energy was contained below 5 cps
and 90% below 30 cps." On that basis, as well as from the
frequency range of interest, the size of the probe tip is
believed reasonable. Also, the shape and location of the pod
containing the transducers is such that its pressure should
not seriously influence the flow field about the tip.

A photograph of the probe components before
assembly is shown in Figure 6. The main body is easily
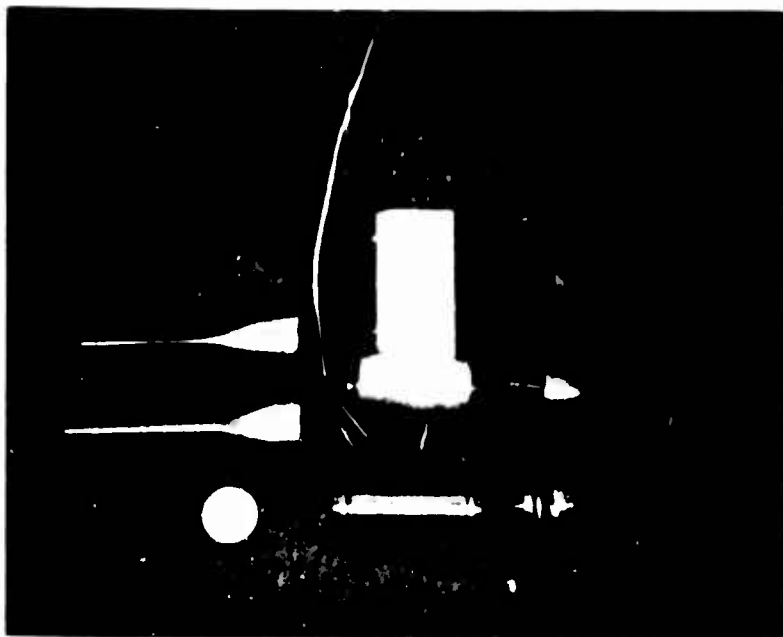
FIGURE 6   PROBE COMPONENTS
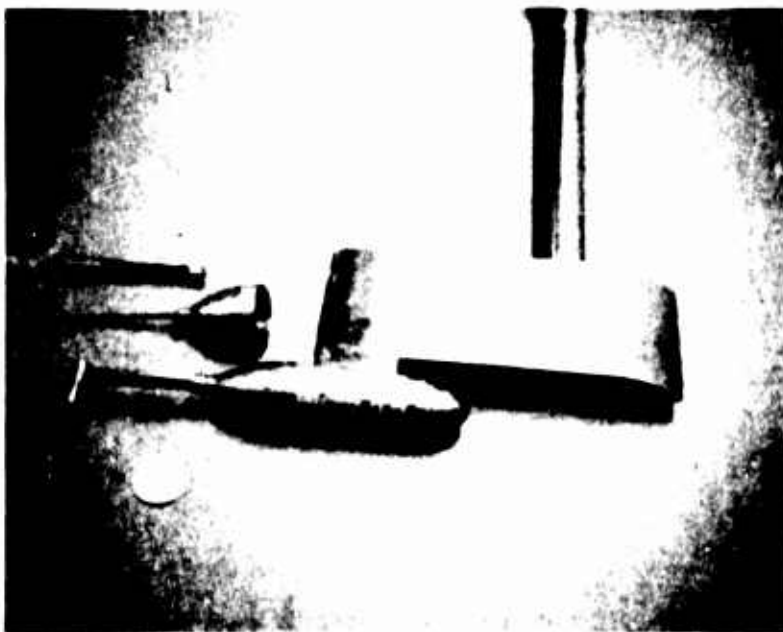
FIGURE 7   FINAL PROBE ILLUSTRATING BOTH HEADS AND THE
SHIELDS EMPLOYED

identified. Below that is the transducer assembly (two transducers epoxied in a support tube). To the right of that assembly is an actual transducer of the type employed. The rear cap of the probe unit is also easily recognized. The remaining probe components are "heads." The upper one illustrates the basic concept which was later modified through the addition of "shields" to isolate the tip from unwanted cross-flow interference. The lower head in the photograph is an early shielded design which did not prove successful.

Figure 7 is a photograph showing the probe as it eventually evolved and was used in these tests. On the probe proper is the head employed for measuring vertical velocity perturbations, while above it is the head used for measuring axial velocity perturbations. The shield used during axial measurements is above the basic axial head unit.

Calibration Techniques

It is recognized that the Bernoulli relationship between pressure and velocity, even in its modified form for unsteady potential flow, will not be appropriate for application to the present problem because of the important effects of viscosity, dissipation, mixing, etc., which occur in a wake. However, it is believed that the calibration techniques employed herein do not depend upon such an

explicit relationship initially. The final interpretation of the data will depend upon such a relation, and that will be described in a later section of the report. The calibration technique relates the probe output to pressure head values obtained from different fluid velocities and/or by varying vertical probe displacement. Essentially, the dynamic calibration was accomplished by impinging, upon the tip of the submerged probe, jets of water traveling at known velocities and known frequencies.

This is much more easily accomplished in a conceptual way than in actual practice. To begin with, and assuming the probe will sense flow disturbances, the jet of water impinging on the probe tip must be laminar. If the jet impinging upon the probe tip is turbulent, the device will sense this turbulence. There is also the problem of "instantaneously" starting and stopping the impinging jet at various frequencies. Lastly, a jet element of water, as it proceeds towards the tip of the probe, will displace water in the fluid field ahead of it, and the fluid field will "fill in" after the passage of the jet element. Both of these latter disturbances will also be detected by the probe if it is doing the job it is supposed to.

In view of the above statements it is readily apparent that if the probe performed as desired, the

development of the calibration techniques became an undertaking in which the above mentioned unwanted "side effects" are minimized or wherein the side effects could be rather conclusively identified as causing a certain type of extraneous response. A complete detailing of all calibration techniques tried and all probe modifications undertaken would result in a rather voluminous report. Since its value would be somewhat nebulous, what is presented here are those items considered as having some general value in aiding others to evaluate the performance of the probe. As such, the developments are not necessarily presented in the chronological order of their undertaking.

The initial studies involved only the response characteristics of the total head transducer, as it was believed a matching of the static head transducer response could be made after an acceptable total head response was achieved. After making this assumption, the initial attempt at determining whether or not the probe sensed flow disturbances was undertaken. The signal from the total head transducer was fed into a Sanborn 650 optical galvanometer recorder system and the traces on the chart paper examined for interpreting the output of the probe. This particular Sanborn unit has a sensitivity 10 times that of a standard unit. Thus, extremely large deflections of the galvanometer

were achieved with very minute pressure changes on the surface of the transducer.

The initial calibration test rig consisted of a submerged jet emitting from a nozzle, and a rotating disk (about $\frac{3}{16}$ inches thick) having holes near its outer radius (see Figure 8). When the holes in the disk were aligned with the nozzle it was believed that a jet of water would impinge upon the probe tip. A flow meter in the line feeding the nozzle afforded a means of determining the average exit jet velocity, while the rotational speed of the disk introduced the desired frequency.

The output signal as recorded by the optical galvanometer indicated flow of a very erratic nature. There were large deflections but the signal trace could most accurately be described as "hash." After several days of modifying and retesting, it occurred that perhaps the impinging jet was turbulent and that the records were actually traces of the turbulent flow in the jet.

To test this hypothesis, it was recalled that a stream of fluid emitting from a circular orifice, such as a hole located in a large thin walled container, is laminar for some 2.5-3 orifice diameters downstream. Therefore, a container with a hole in its side was placed in the test section of the tunnel. By having the elevation of the water in the

ACTUAL CLEARANCE BETWEEN
NOZZLE-DISK AND DISK-
PROBE TIP ABOUT
1/16 INCH

METERED WATER
SUPPLY

ROTATING DISK
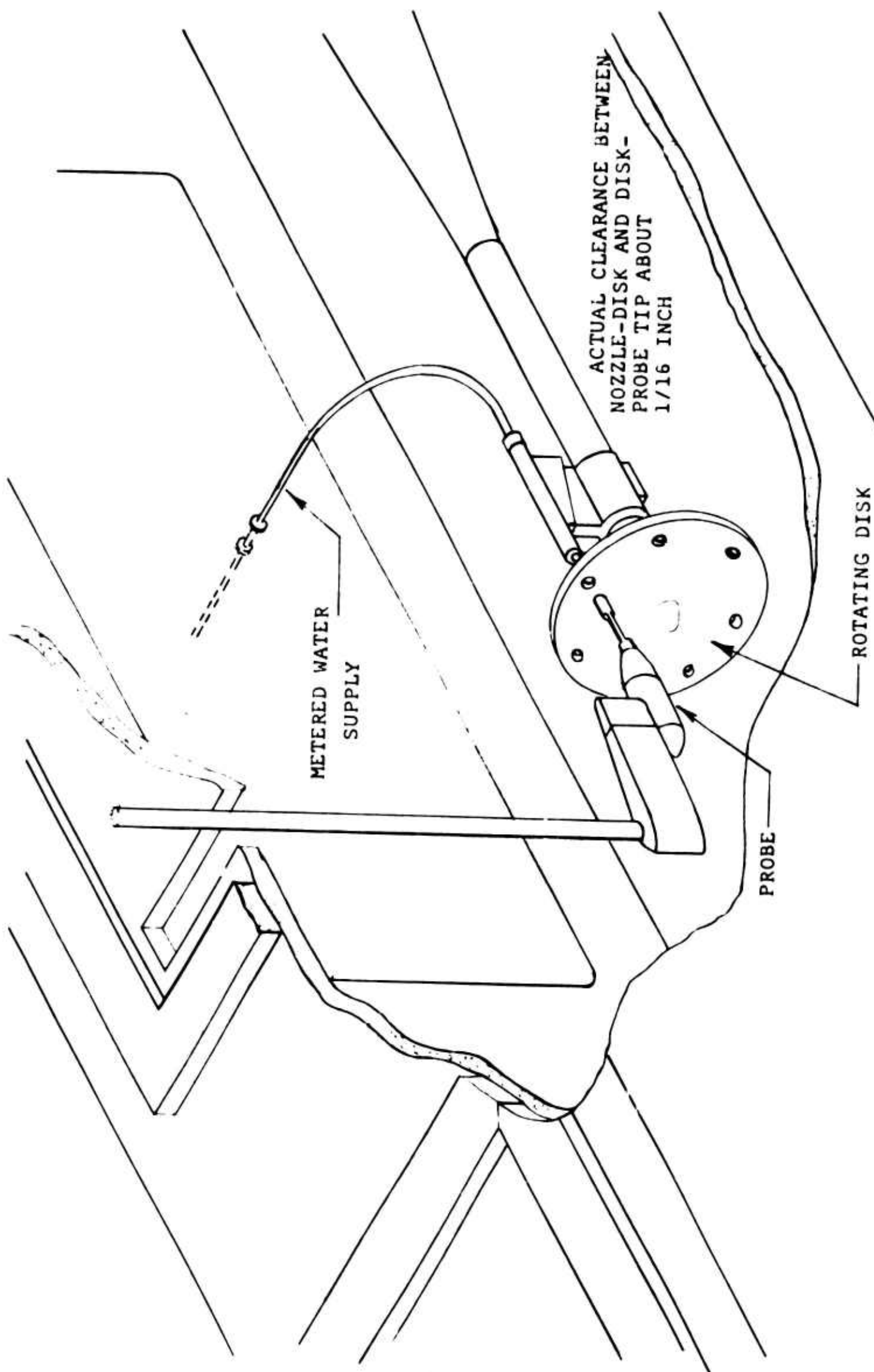
PROBE

FIGURE 8 SKETCH OF INITIAL CALIBRATION RIG

container higher than the level of water in the open test section of the tunnel, the resulting difference in head produced a submerged jet of known exit velocity. The probe was supported on a carriage with the tip at the elevation of the centerline of the orifice (see Figure 9). Moving the tip along the horizontal centerline (extending from the orifice opening to further downstream positions) produced a pattern in the signal output trace which definitely proved the probe sensed disturbances existing in water. In the area within 3 diameters downstream of the orifice opening, the signal was a relatively steady trace and this corresponded to the distance in which a laminar jet should exist. As the probe was positioned at axial distances greater than this, the signal began to undergo large deflections and it also became erratic. This erratic nature of the signal (as well as the deflections) decreased as the probe progressed further and further downstream from the orifice opening until finally the signal level reached the value existing in the stationary fluid field.

A trace of the signal output taken at a later time with both the total and static head transducer signals separately recorded is shown in Figure 10. From tnis figure it can be noted that the static pressure changes slightly near the jet exit before returning to the ambient static pressure. The total or impact level decreases from a maximum

WATER LEVEL IN TANK
HIGHER THAN WATER IN
TEST SECTION THUS
PRODUCING FLOW FROM
ORIFICE.

ORIFICE

CARRIAGE PERMITTING
AXIAL POSITIONING

OCEANICS
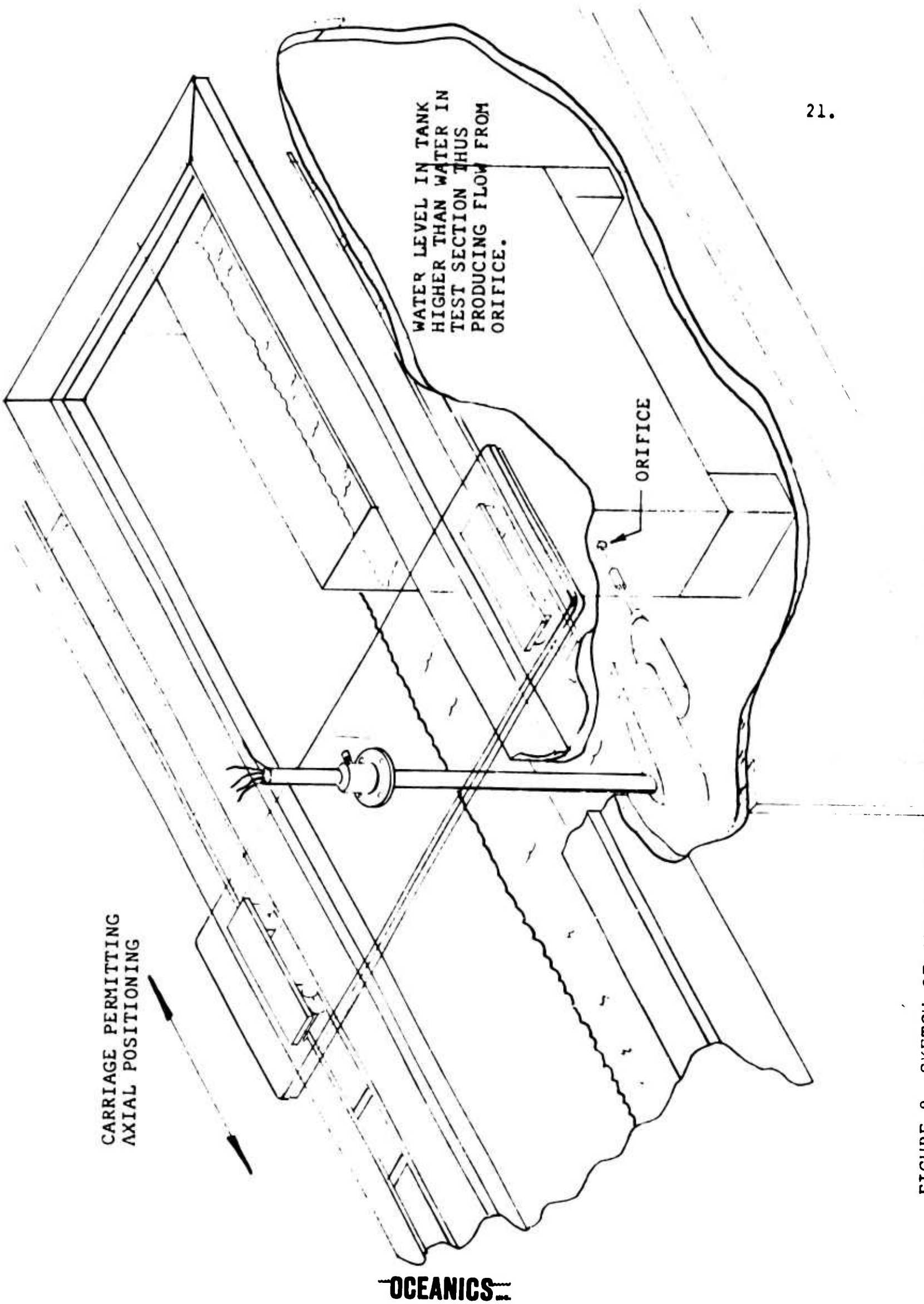
FIGURE 9 SKETCH OF ARRANGEMENT USED IN DETERMINING VELOCITY FLUCTUATIONS IN A FREE JET

ORIFICE DIAMETER: $\frac{1}{8}$ INCH

DISPLACEMENT OF TOTAL HEAD IS DUE TO 4 INCHES OF WATER HEAD

| |← 0.1 SECOND

UPPER TRACE IS TOTAL HEAD
LOWER TRACE IS STATIC HEAD

NO FLOW (AMBIENT)

AT ORIFICE OPENING

$\frac{1}{4}$ INCH SPACING

$\frac{1}{2}$ INCH SPACING

$\frac{3}{4}$ INCH SPACING

$1\frac{1}{2}$ INCH SPACING

3 INCH SPACING

7 INCH SPACING
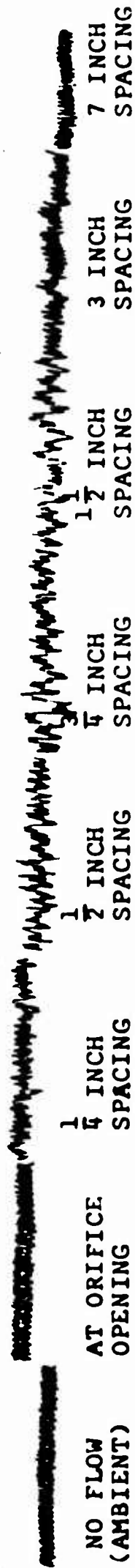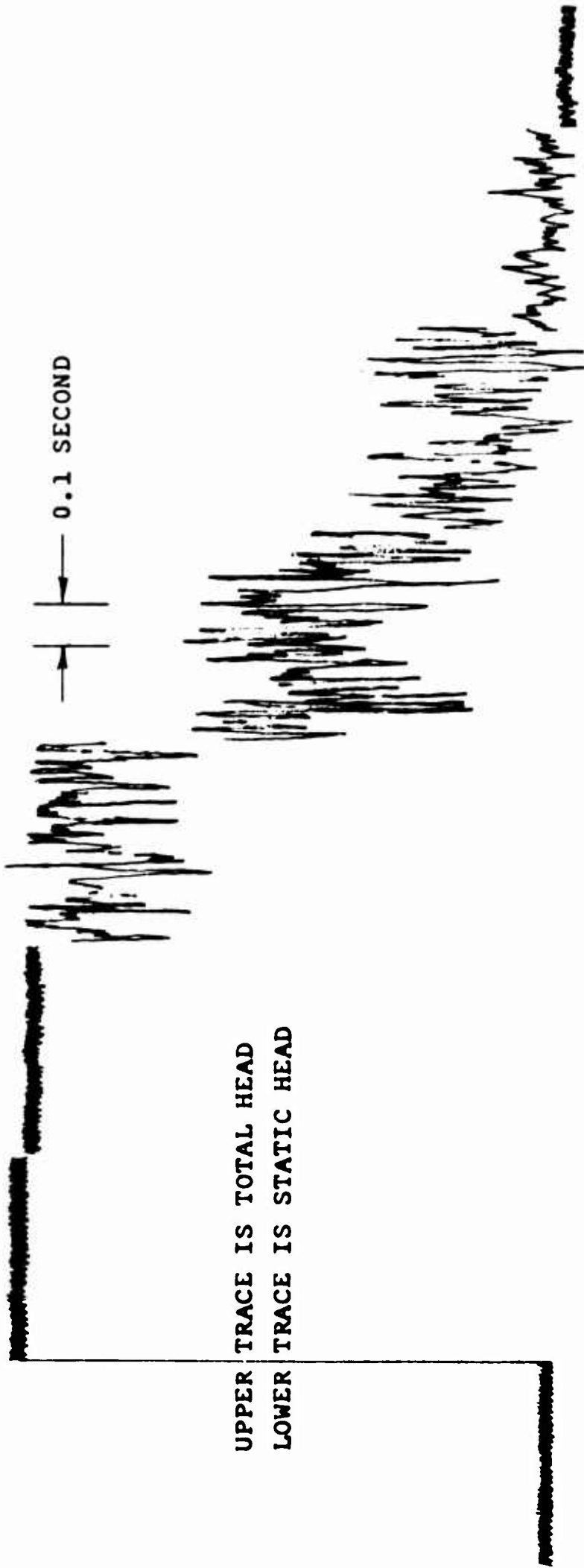
FIGURE 10   TRACES FROM GALVANOMETER RECORDS ILLUSTRATING "TURBULENCE" IN A FREE JET WITH AXIAL DISTANCE

22.

at the orifice opening to the ambient conditions at some distance downstream. The location of the beginning of the disturbed signal agrees well with the end of the laminar conditions. The water level in the container was kept at a constant level during the test run.

Considerably encouraged by this revelation, the next step involved a use of the container with an orifice as the source of the impinging jet, but retaining the rotating disk as a means of interrupting the jet and thus introducing a variation in the frequency of jet impingement. The thickness of the disk in the area containing the holes was reduced to about 0.015 inches, as the thicker disk contained water in the hole passageways and the impinging jet had difficulty forcing this water out. The thicker disk also affected the jet pattern as each hole lined up with the jet stream to a larger extent than did the thiner disk.

It might be well to point out here that a liquid jet issuing from an orifice and interrupted by holes in a disk does not issue forth on the other side of the disk as nice segmented elements (or slugs) of water. Studies of such an interrupted liquid jet (exiting in air) using a stroboscope, clearly showed that the jet on the exit side of the disk does not follow the axial centerline of the orifice but rather spews forth with the jet sweeping through an arc. In

other words, as a very small portion of the hole in the disk is aligned with the beginning of the jet stream, the fluid forced through this partial opening does not exit along the orifice centerline but rather at an angle to the centerline. As more and more of the hole in the disk aligns with the jet, the emitting stream approaches the axial centerline of the orifice and when both the orifice and the hole in the disk are in alignment, the jet is along the orifice centerline. As the hole passes beyond this optimum position, the jet changes its orientation from the orifice centerline and again is discharged at an angle to the orifice centerline. Because the disk is rotating, there is also a boundary layer growth along its surface, with this boundary layer also influencing the jet vector. To minimize this, the disk is run only partially submerged; therefore friction has only a short distance in which to develop a boundary layer and influence the jet vector impinging on the probe tip. The final calibration setup is shown in Figure 11.

At this point it has been established that at least the total head probe detected flow disturbances, and that a fairly satisfactory dynamic calibrating device consisted of a submerged free jet issuing from an orifice with this jet interrupted by a thin disk containing holes. The procedure required the probe tip to lie within the axial

25.

HEIGHT OF WATER LEVEL IN CONTAINER ABOVE TUNNEL LEVEL IS VARIED TO CHANGE JET VELOCITY

DISK-CONTAINER AND DISK-PROBE CLEARANCE IS LESS THAN 1/16 INCH

DISK IS RUN ONLY PARTIALLY SUBMERGED TO REDUCE BOUNDARY LAYER INFLUENCE ON EMITTING JET

OCEANICS
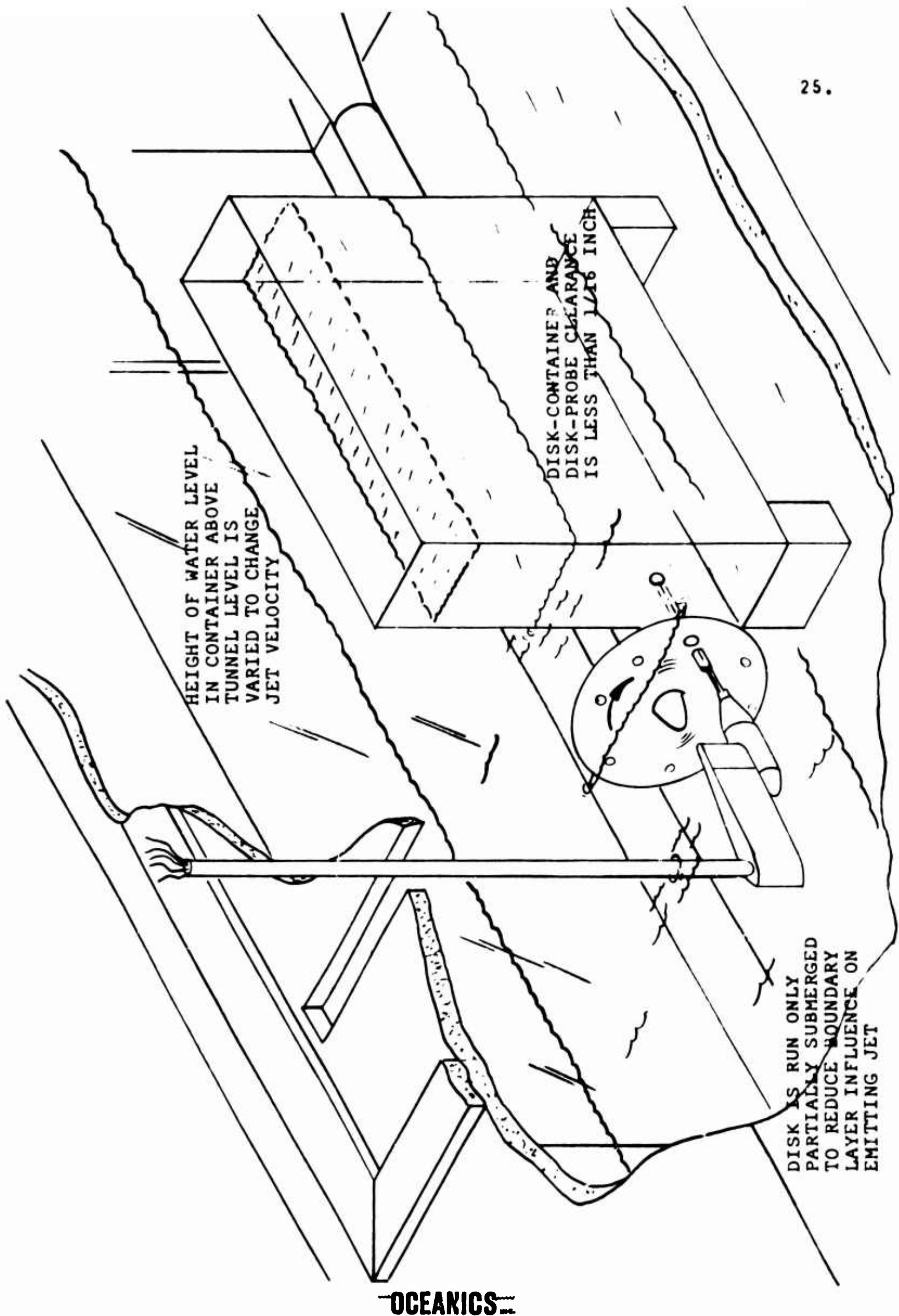
FIGURE 11   FINAL ARRANGEMENT FOR DYNAMICALLY CALIBRATING THE PROBE

distance from the orifice opening wherein the laminar portion of the submerged free jet existed.

The last step required a determination of the best response characteristics obtainable with the total head portion of the probe, followed by a matching of the static head response to this criteria. The best response was determined by the ability of the sensing unit to produce a square wave output signal when the probe was placed in the laminar jet and the jet interrupted by the rotating disk. (It must be recognized from earlier discussion that a perfect square wave is not possible because the fluid cannot be started and stopped instantaneously.) What was desired was a constant amplitude output regardless of frequency (for a given jet exit velocity) with the amplitude value following some repeatable relationship with the calculated jet exit velocity.

The internal diameter of the tube was perhaps the most important parameter. While the instrument described in [4] considered the mass of water in the diaphragm well and the mass of the diaphragm negligible compared to the effective mass of the water in the impact tube, in this probe there was very little mass of water in the impact tube compared to the mass of water in the diaphragm well. The results of the tests of the instruments described in [4]

also state that the effect of viscous damping is small. In our case, it was believed that the viscous effect of the fluid moving in the tube was the principal factor in changing the frequency response characteristics. For example, changing the interior tube diameter by only several thousandths of an inch brought about marked changes in the response, while the total mass of water contained in the system was changed very little (although the mass of liquid in the tube itself was changed significantly). Also, filling the diaphragm well and tube with light oils caused a reduction of the order of two magnitudes in the frequency response of the system!

The length of the tube was also varied, although the range of length variation was somewhat limited as the tube had to remain stiff enough so that its natural frequency remained high enough (thereby not influencing the output of the probe). Here also it appeared as if the viscous effects of the fluid far outweighed the change of mass in the system.

Once the interior tube diameter and length of the total head sensing portion of the probe were established (see Figure 5), the response of the static head transducer had to be matched to it. The matching had to be exact in terms of frequency response as the static head signal is subtracted from the total head signal. Exact amplitude response

matching, while desirable, was perhaps not necessary as the final calibration of the unit would be done with the signals subtracting. Fortunately, it was possible to match the output signals from the transducers from both frequency response and amplitude considerations by adjusting the outer tube's internal diameter as well as the size of the static pressure openings. The water volume contained in the end cap of the probe proper was also reduced from that of the original design.

The matching of the transducer responses was established in a relatively simple manner. The output of each transducer was fed into a separate channel on the optical galvanometer. The probe was oriented in a horizontal manner, i.e. the longitudinal axis of the probe was horizontal. Then the entire unit was submerged in the open test section of the tunnel. In this condition, both transducers were subjected to the static head existing at a given depth of submergence. By changing the depth of submergence the pressure on both transducers was varied in an identical manner. Thus the output of both transducers should remain identical. The traces of a rapidly moving up and down probe should thus remain as two parallel lines, these lines maintaining the same differential distance between them that existed with no velocity regardless of the frequency of the vertical motion.

A trace taken from one of the optical galvanometer records made with a shielded probe (i.e. a final calibration) is shown in Figure 12. Here it can be noted that both transducer outputs retained the same relationship with one another regardless of frequency.

The last major problem involved shielding the tip of the probe in some manner so as to insure that flows occurring at any direction other than that in which measurements were desired did not introduce erroneous outputs. This was particularly important because measurements were desired of the vertical velocity fluctuations wherein the main free stream flow would be passing perpendicular to the tip of the sensing element.

The probe tip to be used for axial measurements was tackled first, as it was believed that a solution to this portion of the problem would then permit a relatively easy adaptation for the vertical measurement requirements. It was believed that a shield, formed from a section of tubing, and placed over a portion of the tip would prevent cross-flows from interfering in an adverse manner with the sensed values. It was also important that the shield not affect the response characteristics of the probe. The final shapes of the shields employed during the studies were shown earlier in Figure 5.
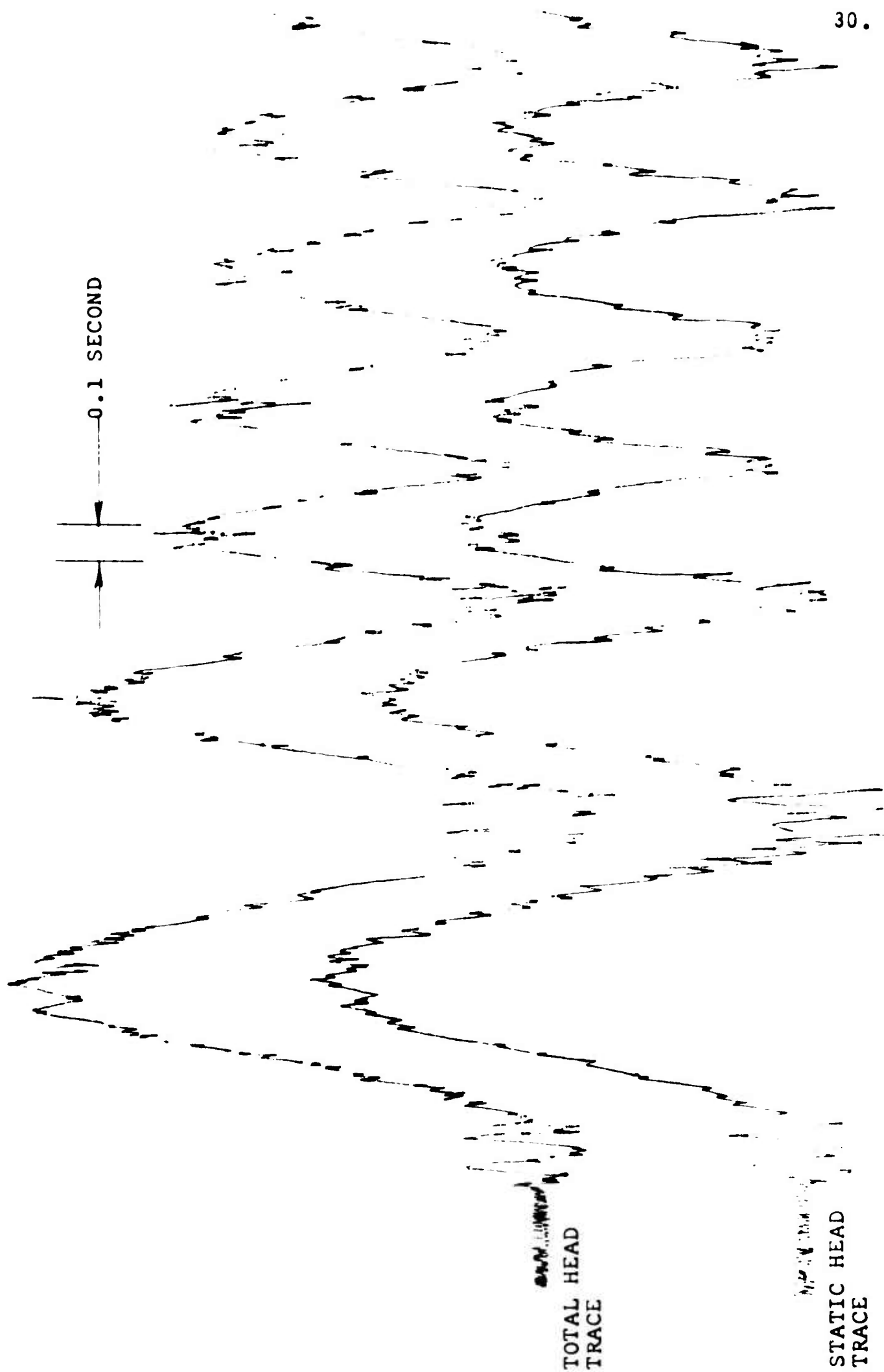
FIGURE 12   TRACE OF OPTICAL GALVANOMETER ILLUSTRATING RESPONSE OF
BOTH TRANSDUCERS WITH VARYING PRESSURE HEAD AND FREQUENCY

To test the performance of the shield, the unit
was placed in a laminar jet and then oriented at different
angles to the laminar jet. In other words, measurements of
the probe output were taken with the probe oriented with
the laminar jet and at various angles of rotation until the
tip was oriented 90° or perpendicular to the laminar jet.
When the tip was oriented perpendicular to the laminar jet
the output signal should remain the same as for a zero flow
condition. How well the shield worked is shown in Figure 13,
which shows traces taken from optical galvanometer records.
From the traces on this figure, it can be noted that the
probe was insensitive to angular orientation, i.e. it sensed
the true jet velocity for angles up to 20° when the flow
was impinging directly upon the probe tip and to 30° when
the flow was at right angles to the probe tip.

It was, in fact, this latter development which
lead to the development of the probe head used for detecting
vertical velocity fluctuations. Originally it was planned to
change the orientation of the probe unit such that for ver-
tical measurements the entire unit would be rotated 90° from
that employed for measuring the axial fluctuations velocities.
However, it was found that with the unit oriented at 90° the
response suffered due to gravity acting on the water mass in
the diaphragm wells, which had a pronounced effect on the
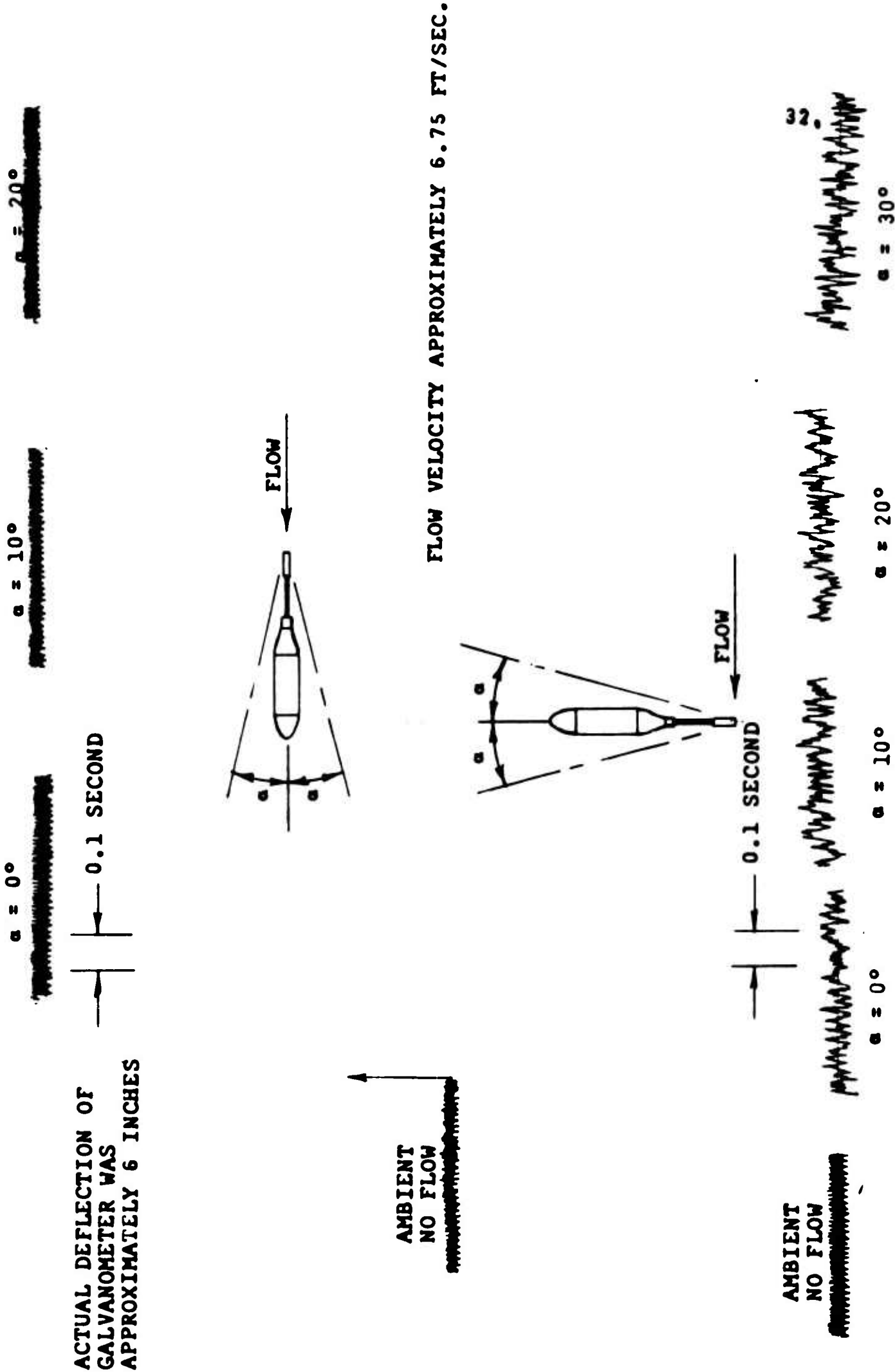
FIGURE 13   TRACES OF OPTICAL GALVANOMETER RECORDS ILLUSTRATING THE
EFFECT OF FLOW ANGLE ON PROBE RESPONSE

signal output, whereas the gravity effect was negligible with the probe oriented in the manner for taking axial measurements.

Taking note of how effective the shield was in preventing cross flows from affecting the probe output, i.e. when the probe was oriented perpendicular to the main stream, it became apparent that if the probe tube was bent 90°, and then shielded, the unit would undergo none of the disadvantages due to gravity effects (on the diaphragm chamber water masses) influencing the response characteristics. The only question which arose was whether a bend in the tube would affect the response of the unit. Putting a bend in the tube and orienting the tip 90° from its orientation used in vertical measurements did not effect the response, and therefore the evolution process of the two heads was completed.

Before concluding the discussion of probe development, the effect of air in the system should be mentioned. The elimination of air trapped in the diaphragm well of the probe was stated as being of major concern in [4]. Therefore, the probe employed in these studies was specifically designed to permit assembly while minimizing the probability of entrapping air in the system. The assembly procedure was as follows.

1- Both the head and end caps were removed from the probe.

2- The unit containing the transducer assemblies was
then submerged in the tunnel.

3- A jet of low velocity water was then played about the
face of the transducers forcing water through the
passageways about the transducer assembly and the ex-
ternal pod shell. With this flushing action, all air
bubbles weᵢe removed from that portion of the unit.

4- Keeping the transducer unit submerged, the end cap
was next submerged and the jet of water used to flush
it free of any air bubbles. The end cap was then
screwed on the transducer unit.

5- The head unit was then submerged. The size of the
head was such that by holding it in your hand, placing
your thumb over the threaded end and then compressing
the water trapped in the diaphragm chamber with your
thumb, water was forced from the diaphragm chamber out
the sensing tubes. This procedure was repeated perhaps
a dozen or so times, keeping the unit submerged, to be
sure all air bubbles had been flushed from the system.

6- Keeping all units submerged, the head unit was then
screwed on the transducer unit thus completing the
assembly operation.

Any air in the system was readily noticed, as the

response characteristics of the transducers changed markedly. Figure 14 is a trace taken from optical galvanometer records illustrating the difference in the response signal with and without air in the system.

As a final item, several examples of traces taken from optical galvanometer records illustrating the frequency response characteristics will be presented. These are shown in Figures 15, 16, and 17. On these figures the response of the instrument at various jet exit velocities and frequencies can be noted. At very low frequencies the output signal is quite close to a square wave. As the frequency is increased, the slight increase in the signal above the "steady" laminar velocity value and the dip of tne signal below the steady ambient value is believed due to the manner in which the element of jetting liquid actually impinged upon the probe tib. A discussion of the impinging jet as it was interrupted by the disk was given earlier.

TEST PROCEDURES

The arrangement of the model in the tunnel and the general positioning of the probe along the glide path was discussed in the section on Test Arrangement. During testing, this arrangement was maintained while the probe was positioned

FIGURE 14   RESPONSE CHARACTERISTICS OF PROBE WITH AIR BUBBLES IN THE PROBE UNIT
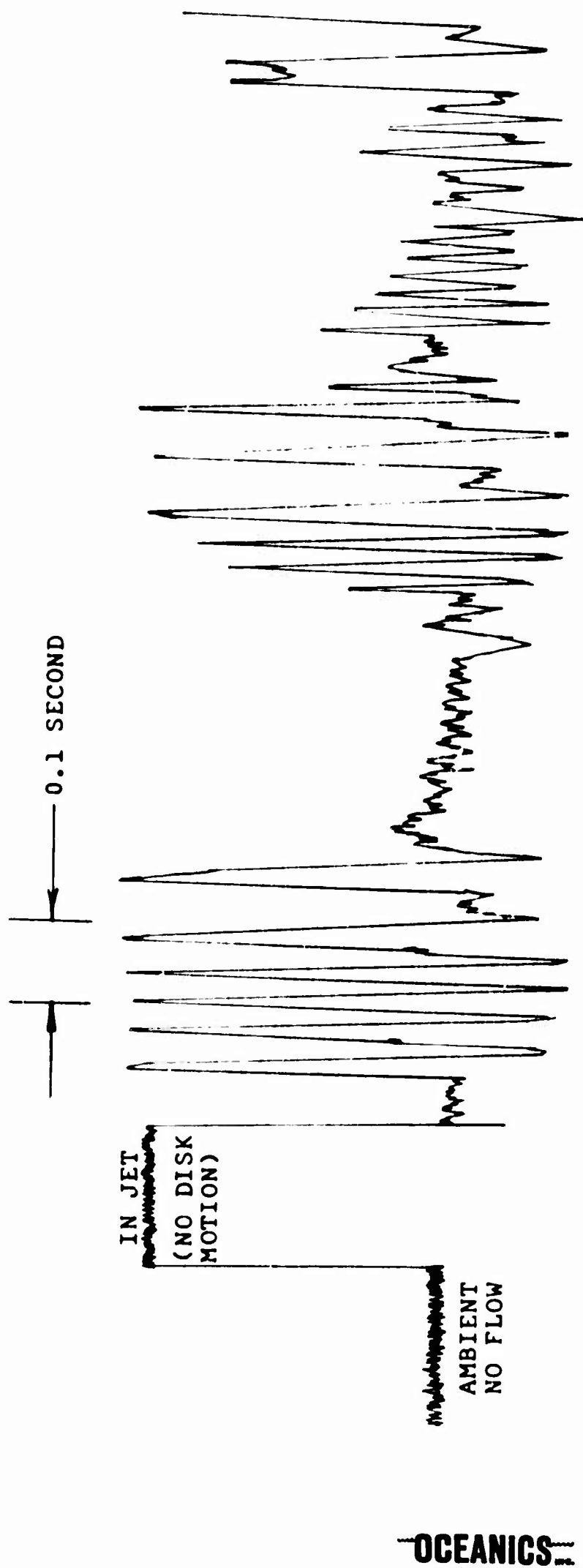
COMPARE WITH FIGURE 15 OR 16 FOR RESPONSE OF UNIT COMPLETELY FILLED WITH WATER
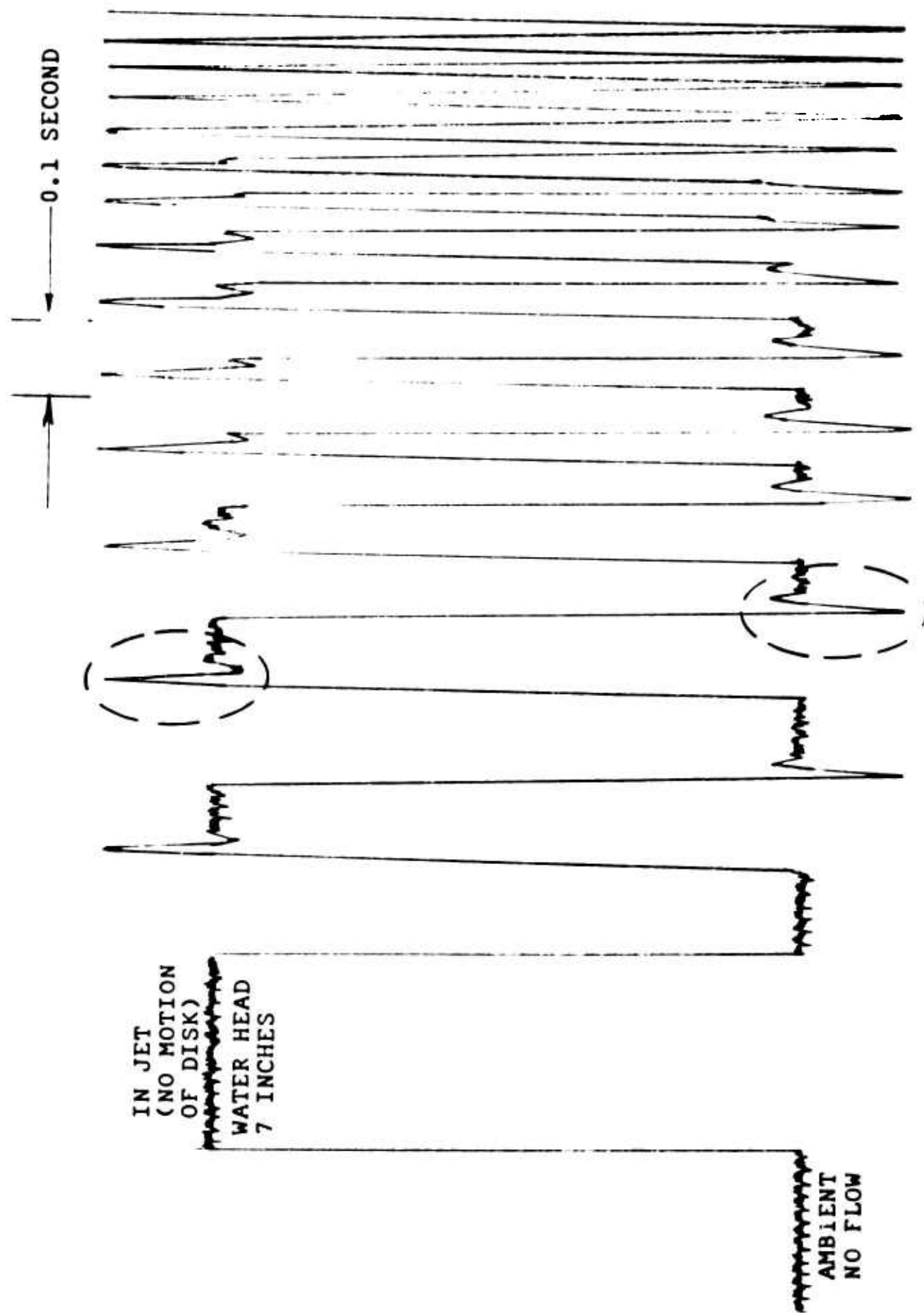
THE RISE AND DIP SHOWN IN THE RESPONSE CURVE ABOUT THE "STEADY"
VALUES IS BELIEVED DUE TO THE JET EMISSION AS THE ORIFICE IN THE
DISK ENTERS AND EXITS FROM THE JET. (REFER TO TEXT AND FIGURE
17 FOR FURTHER DISCUSSION OF THIS PHENOMENON)

FIGURE 15   DYNAMIC RESPONSE CHARACTERISTICS OF THE PROBE FOR A
            WATER HEAD OF 7 INCHES
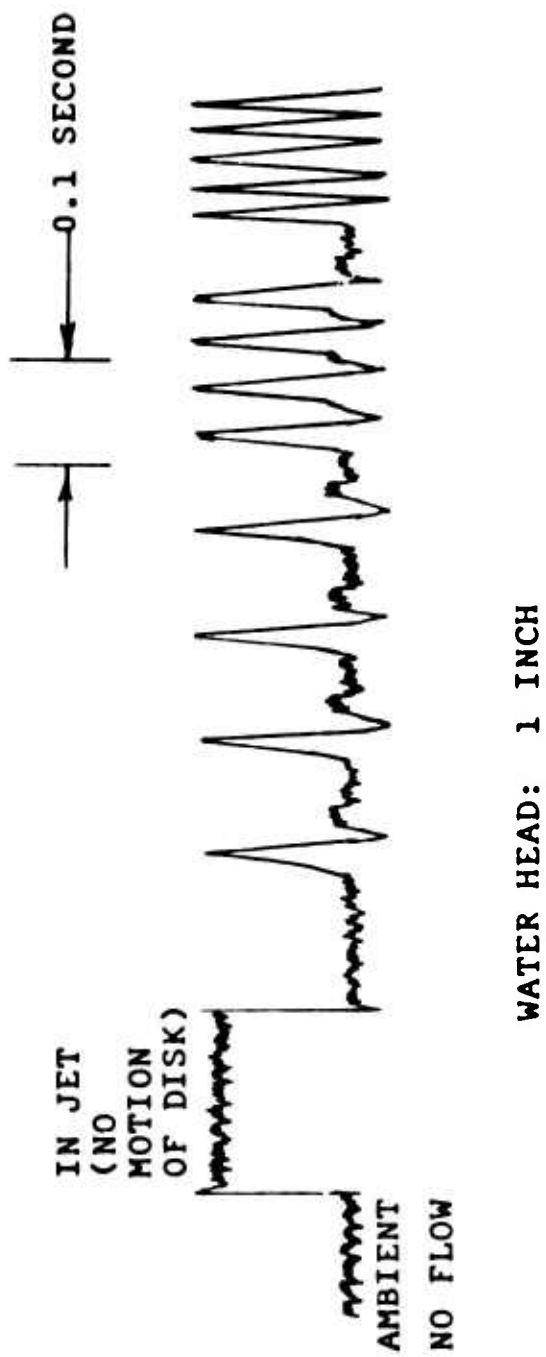
WATER HEAD: 1 INCH

FIGURE 16   DYNAMIC RESPONSE CHARACTERISTICS OF THE PROBE FOR A
WATER HEAD OF 1 INCH

NOTE: THIS DISK CONSISTED OF 3 HOLES, A RADIAL SLOT, 3 HOLES, ETC., RATHER THAN ONLY EQUALLY SPACED HOLES

0.1 SECOND

IN AIR JET
(NO MOTION
OF DISK)

AMBIENT
NO FLOW
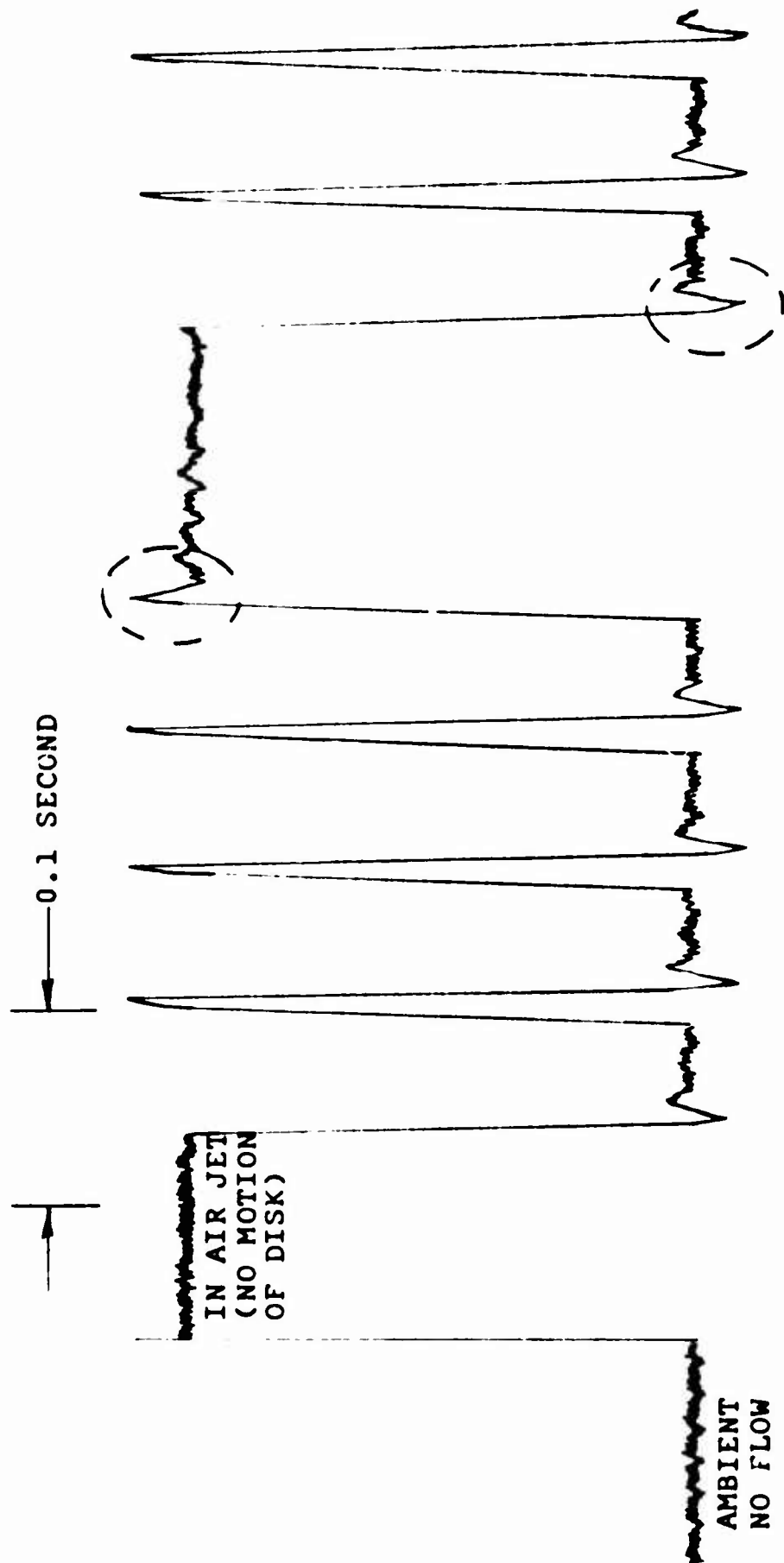
THIS TRACE WAS ACHIEVED USING AIR RATHER THAN WATER AS THE TEST MEDIUM; I.E. NO WATER IN THE PROBE UNIT, THE UNIT SUSPENDED IN AIR, AND AN AIR JET BEING INTERRUPTED BY THE ROTATING DISK. THE SAME RISE AND DIP IN THE RESPONSE CURVE CAN BE NOTED HERE AS ON FIGURE 15, OFFERING ADDITIONAL CORROBORATION THAT THIS CHARACTER-ISTIC OF THE PROBE RESPONSE IS DUE PRIMARILY TO THE CALIBRATION PROCEDURE AND NOT THE MASS OF THE WATER IN THE UNIT

FIGURE 17 RESPONSE CHARACTERISTICS OF THE PROBE IN AIR

OCEANICS

at various locations in the glide path area.

Dynamic Velocity Measurements with Carrier Motion

For dynamic measurements, the probe was positioned at glide path angles of 3°, 4° and 5°. Measurements were made on the glide path and at positions equivalent to 47 feet port and starboard of the glide path centerline. (The 47 foot dimension was selected as a reasonable distance about the centerline of the glide path wherein flow conditions should be studied to gain representative information for simulator studies.) Thus a matrix of nine measuring points at each axial station was formed. This was the same matrix of points investigated for steady values and reported in [2]. The axial distances also corresponded to those investigated for steady flow values and were equivalent to distances of 226 ft., 485 ft., 764 ft., and 1040 ft. aft of touchdown. (For CVA 62, 64 and 65 class carriers, touchdown is assumed to be 150 ft. ahead of the trailing edge of the ramp-see DTMB Aero Rept. 955, Parts I, II and III.)

The model was oriented in the tunnel so that the wind direction (ψ) relative to the keel of the ship was 10° and 3° port. With the 10° angle, the "wind" direction was parallel to the centerline of the landing deck. The 3° angle was selected on the basis of having the "wind" direction as close as possible to the keel-line, while permitting the model to be positioned in the tunnel such that meaningful measurements would be taken

downstream. With the model aligned in the test section having the keel parallel to the oncoming "wind", an extension of the glide path from the landing deck extended through the tunnel walls (due to the angle of the landing deck) before the desired downstream measuring distances were obtained.

The signal from the probe went to the Sanborn amplifier, then through a Krohn-Hite variable bandpass filter set at the appropriate centerband frequency*, and from there to a Beckman recorder. Also fed into another channel on the Beckman recorder was the output of a linear transducer attached to one actuation rod. In this manner a trace of the ship pitch angle orientation in relation to the probe signal was obtained permitting a determination of phase relations. A schematic of the electrical system is shown in Figure 18.

Actual data taking procedures were as follows:

1. The probe was located at the desired station.

2. The probe output was balanced (strain gage circuitry).

3. The tunnel was started and brought to the proper test velocity.

4. The actuation system was set at the desired frequency.

5. The variable bandpass filter set at the centerband

---

*At centerband settings, the bandwidth of the filter at the 3db down points is equivalent to a range from 0.77 to 1.3 times the setting.
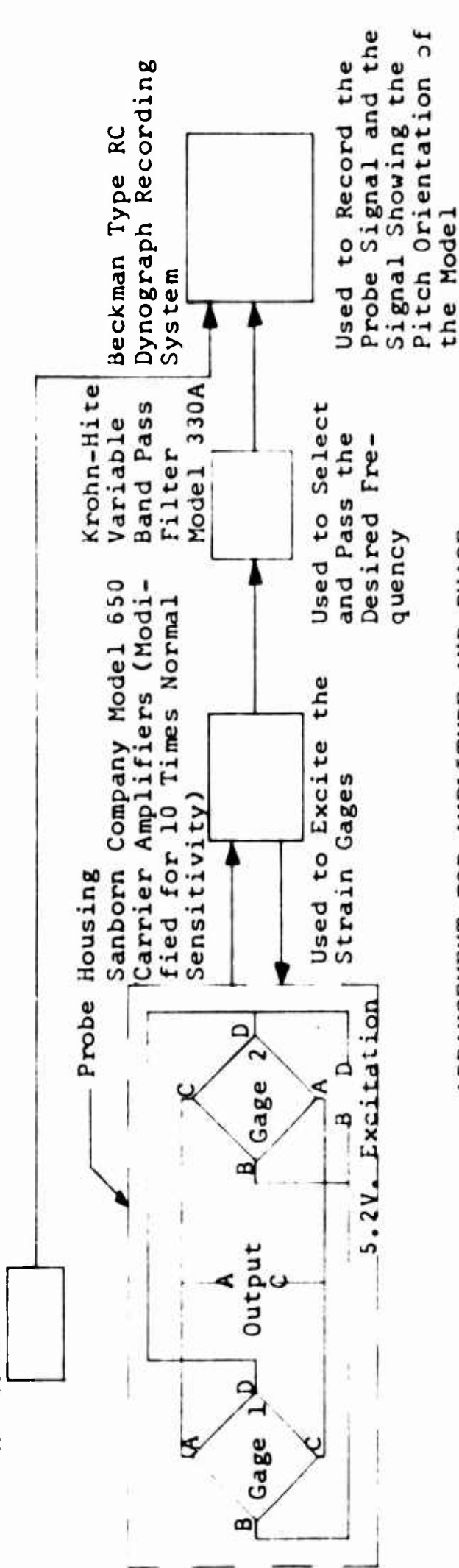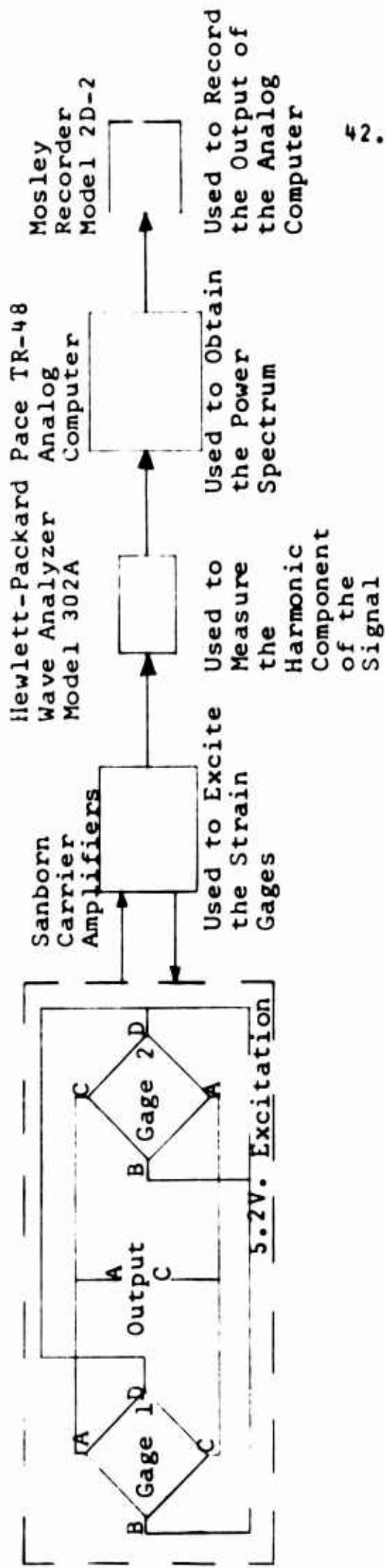
FIGURE 18 SCHEMATIC DIAGRAM OF ELECTRICAL INSTRUMENTATION ARRANGEMENT

frequency corresponding to the actuation system
frequency.

6. The level adjusted on the Beckman recorder (the pens were
centered on the appropriate chart strip).

7. With the model horizontal and with no motion, a trace of
the probe output was taken on the Beckman.

8. With the model in motion, a trace of the probe output
was taken (the sensitivity on the Beckman was adjusted
to obtain the maximum allowable pen deflection).

9. The actuation frequency was changed and the filter fre-
quency changed; then steps 6 through 8 repeated.

10. Step 9 repeated for each of the four pitch frequencies
investigated.

The above procedure was repeated for the taking of
both horizontal and vertical velocity fluctuations for the
following conditions.

1. Two wind orientations ($\psi=3°$ port, $\psi=10°$ **port**).

2. Five pitch frequencies (full scale $\omega=0$, 0.468, 0.607,
0.76, 1.013).

3. Three glide paths (3°, 4°, 5°).

4. Three positions about each glide path (centerline,
47 ft. port, 47 ft. starboard - full scale).

The traces obtained from the Beckman recorder were
of excellent quality and illustrated strong periodicity

which could be related to the ship pitch motion whenever the perturbing velocity had any reasonable magnitude. Figures 19 and 20 are photographs of several typical traces and the strong periodicity of the fluctuating probe output is clearly evident in these traces. The trace corresponding to the ship pitch is also shown.

Dynamic Velocity Measurements Without Carrier Motion

As a further aid in providing input data for the computer studies undertaken by Systems Technology, Inc., estimates of power spectra of the wake were obtained without carrier motion. These studies were undertaken with the same general test arrangement as for the studies with carrier motion, except that measurements were taken only along the centerline of the glide paths of $3°$, $4°$ and $5°$. The process of recording the signal was slightly different for these studies than for that employed for studies with model motion. In this case the signal from the probe went to the Sanborn carrier amplifier, through a Hewlett-Packard wave analyzer, from there to an analog computer where the signal was squared and then integrated for 40 seconds to obtain a long term mean square value of the pressure perturbations. It was this result that was then employed in determining the power spectra. (An outline of the methods of converting such pressure data into useful velocity information will be

UPPER TRACE IS PROBE SIGNAL. MAXIMUM SIGNAL IS UP. 1cm = 50 MILLIVOLTS OF SIGNAL.
(VELOCITY PERTURBATION 7.6% OF FREE STREAM VELOCITY)
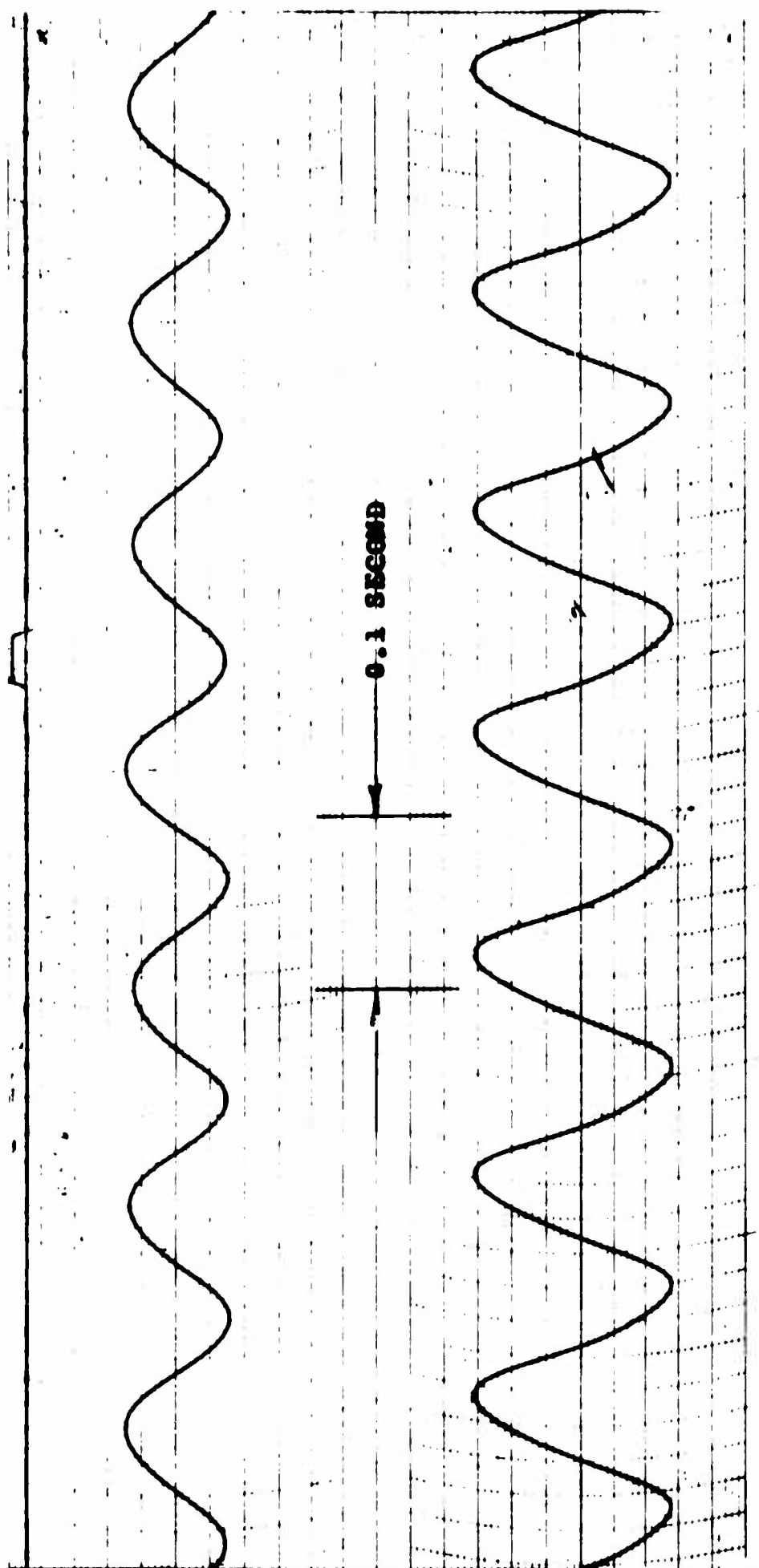
LOWER TRACE INDICATES MODEL PITCH ORIENTATION. POSITIVE PITCH IS UP.

CONDITIONS: 226 FEET AFT OF TOUCHDOWN; 47 FEET PORT OF GLIDE PATH CENTERLINE
GLIDE PATH ANGLE 4°; WIND 10° PORT
MODEL FREQUENCY 7.92 cps; FULL SCALE ω = 0.76

FIGURE 19 BECKMAN TRACES: DYNAMIC HORIZONTAL VELOCITY FLUCTUATIONS

0.1 SECOND

OCEANICS

UPPER TRACE IS PROBE SIGNAL. MAXIMUM SIGNAL IS UP. 1cm = 10 MILLIVOLTS OF SIGNAL. (VELOCITY PERTURBATION 4.8% OF FREE STREAM VELOCITY)
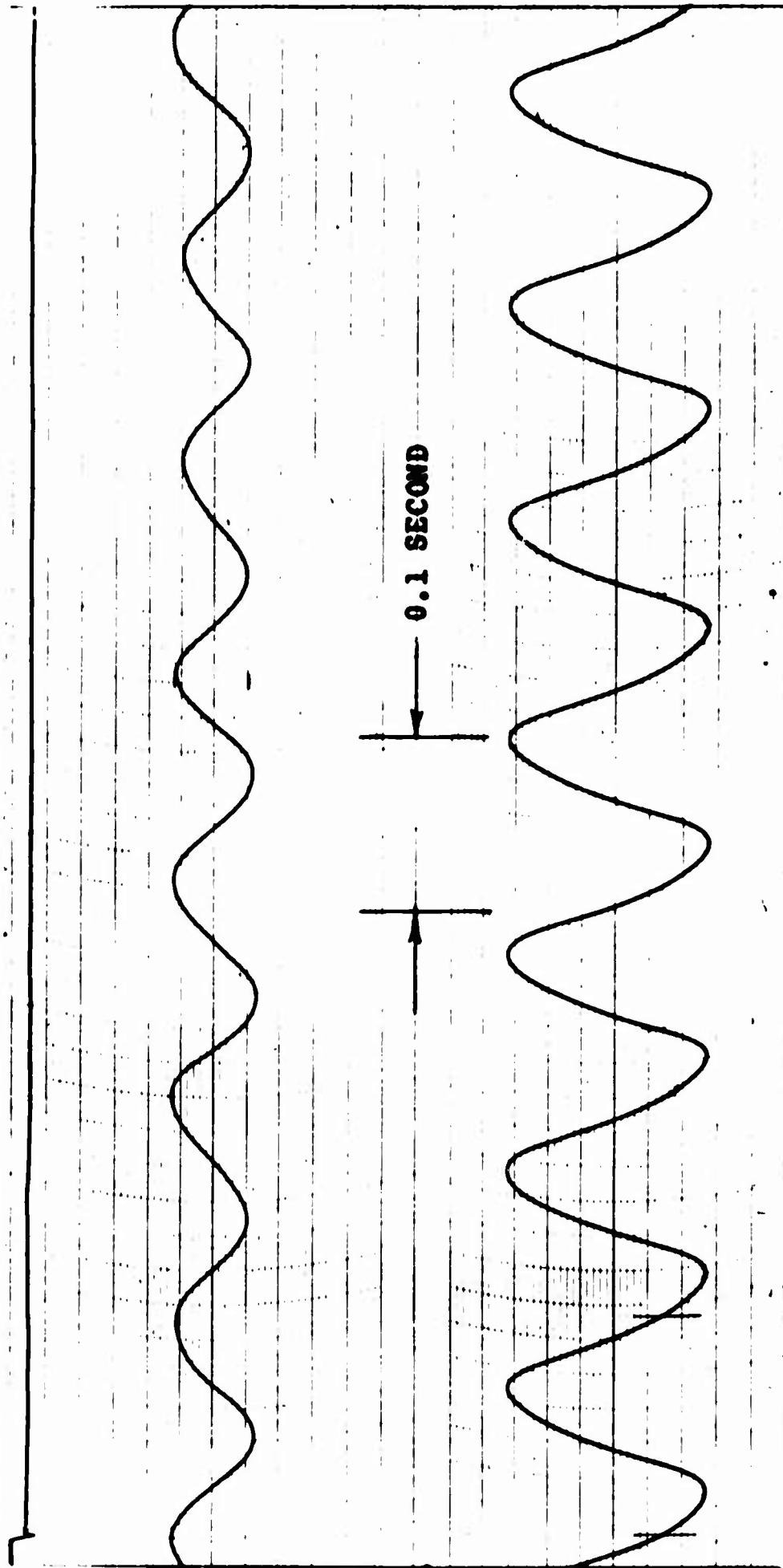
LOWER TRACE INDICATES MODEL PITCH ORIENTATION. POSITIVE PITCH IS UP.

CONDITIONS: 764 FEET AFT OF TOUCHDOWN: ON GLIDE PATH CENTERLINE
GLIDE PATH ANGLE 4°; WIND 10° PORT
MODEL FREQUENCY 7.92 cps; FULL SCALE ω = 0.76

FIGURE 20 BECKMAN TRACES: DYNAMIC VERTICAL VELOCITY FLUCTUATIONS

presented in the next section of this report.) A larger full
scale ω range was investigated here than for the case for
carrier motion, covering ω values (full scale) from .48 to
3.8.

DATA EVALUATION

In the preceding section the procedures employed
for obtaining test data were presented. This section will
be devoted to a discussion of the methods employed and the
reasons for employing such methods in determining the mean
motion and the fluctuating motion of the flow in the wake.
There were two basic methods employed in interpreting the
data; one having to do with carrier motion, the other with-
out. In addition, the axial and vertical velocity fluctuations
required different evaluation techniques.

The basic relations between pressure and velocity
in an unsteady flow, including the effects of viscosity,
are expressed by the Navier-Stokes equations. These equations
are represented in vector form by

$$\rho \left[\frac{\partial \vec{v}}{\partial t} + (\vec{v} \cdot \nabla \vec{v}) \right] = -\nabla p + \mu \nabla^2 \vec{v} \qquad (1)$$

where μ is the dynamic viscosity and the usual interpretation

of the ∇-operator is understood. In the case of flows which
are "turbulent" in nature, as in the present case, the
velocity and pressure are represented as the sum of an
average quantity and a fluctuating quantity (about that
average value level). The average values are those obtained
by standard steady-state techniques, and for the aircraft
carrier wake problem they have already been obtained pre-
viously and reported in [2].

Representing the velocity vector and the pressure
in the form

$$\vec{v} = \vec{V}_a + \vec{v}' \quad , \quad p = P_a + p' \tag{2}$$

where the a-subscripts represent average values and the
primes represent fluctuations, Equation (1) can be expanded
and separated into its separate components for flow along
the axial, vertical and transverse directions. Considering
only the case of axial and vertical flows; neglecting all
cross-flow velocities relative to the probe orientation (the
effect of the shield); and subtracting the average flow
equations, results in the expressions

$$\rho \left[\frac{\partial u'}{\partial t} + \frac{\partial}{\partial x}\left(U_a u' + \frac{u'^2}{2}\right) \right] = - \frac{\partial p'}{\partial x} + \mu \nabla^2 u' \tag{3}$$

for axial flow, and

$$\rho\left[\frac{\partial w'}{\partial t} + \frac{\partial}{\partial z}\left(W_a w' + \frac{w'^2}{2}\right)\right] = -\frac{\partial p'}{\partial z} + \mu\nabla^2 w' \qquad (4)$$

for vertical flow, where u' and w' are the axial and vertical velocity perturbations, respectively, and similarly for U_a and W_a in regard to average values. Integrating Equation (3) with respect to axial distance x from the probe tip x_1 up to the point x_2, corresponding to the location of the probe static hole, leads to

$$P'_{total} - P'_{static} = \Delta p' =$$

$$\rho\int_{x_1}^{x_2}\frac{\partial u'}{\partial t}dx + \rho\left(U_a u' + \frac{u'^2}{2}\right)\Big|_{x_1}^{x_2} - \mu\int_{x_1}^{x_2}\nabla^2 u' dx \qquad (5)$$

This result may be considerably simplified by assuming only small spatial variation of the velocity u over such a small distance as the separation between the two probe holes; stagnation conditions (u=0) at the probe tip; and a sufficiently high Reynolds number such that the viscous term may be neglected. This leads to

$$\Delta p = \rho\Delta x\cdot\frac{\partial u}{\partial t} + \rho\left(U_a u + \frac{u^2}{2}\right) \qquad (6)$$

for the axial case, and by a similar procedure to

$$\Delta p = \rho\Delta z\frac{\partial w}{\partial t} + \rho\left(W_a w + \frac{w^2}{2}\right) \qquad (7)$$

for the vertical case, which are the fundamental relations that were used in the data analysis (prime notation on the fluctuations is now dropped for simplicity in expression). Although it is recognized that the foregoing analysis is extremely simplified and depends on the validity of many broad assumptions, the final relations can be considered indicative of the major contributions to the pressure-velocity relations in the present complex flow problem. Subsequent to the development of these relations, further support for the axial flow relation was obtained by discovery of a result in a paper by Corcos [5] wherein the predominant part of the pressure signal was found to be the same as that in Equation (6). Thus the relations in Equations (6) and (7) may be viewed as reasonable approximations, and the data analysis could proceed on that basis.

The initial application of these results was to the case of carrier pitch oscillation, where a periodic motion was introduced to the carrier. With such a predominant forcing motion, the major effect in the probe output (i.e. pressure signal) would be the periodic component. Upon passing the signal through the Krohn-Hite filter and recording the output on the Beckman pen recorder, this expectation was verified. Examination of Equation (6) showed a negligible contribution of the $\rho\frac{u^2}{2}$-term to the resultant

signal, due to the small magnitude of this term relative to $\rho U_a u$ and also the fact that a u^2-term produces a second harmonic contribution. Similarly the time derivative term $\rho \Delta x \frac{\partial u}{\partial t}$ produces a periodic output that is 90° out of phase with $\rho U_a u$, and which is somewhat smaller than this pure velocity perturbation, in the ratio $\frac{\omega \Delta x}{U_a}$, which produces a phase shift ($\tan^{-1} \frac{\omega \Delta x}{U_a}$) and amplitude increase of the resultant pressure signal. However for the frequencies, forward speed, and probe dimensions in the present program, the phase shift was at most 7° and the amplitude increase less than 2%. Therefore, for all practical purposes in this part of the program, the pressure signal may be approximated by its predominant portion as

$$\Delta p \approx \rho U_a u \qquad (8)$$

in view of the resolution possible in reading the recorder data.

Referring to the calibration curves, with reference to the average conditions corresponding to an axial velocity U_a, the perturbation pressure level (in conjunction with Equation (8)) will allow an evaluation of the axial perturbation velocity u. (The average pressure levels, converted to average axial velocities, were obtained independently from voltmeter readings during the tests. These values were found to be essentially the same as the values obtained in

the steady-state tests of [2], thereby providing further support for the basic test and analysis procedure, and also establishing a link between the steady-state and time-dependent flow fields.) The phase of u (or the pressure signal from the probe) relative to the ship pitch angle is determined directly from the filtered output on the Beckman recorder (the filter was set for zero phase shift), and thus a transfer function between axial perturbation velocity and ship pitch can be constructed.

The amplitude of this transfer function is the ratio of the nondimensional axial velocity perturbation (nondimensionalized by dividing by the oncoming free stream velocity, corresponding to the wind-over-deck velocity) to the pitch angle (in radians).

Only one pitch angle, viz. 1.5° amplitude, was used in this study, due to limitations in time and effort in this program, and hence it was implicitly assumed that the transfer function was linear with pitch angle amplitude. The transfer function was obtained for various frequencies over the range in which ship pitch motion was significant. These results, expressed in terms of full scale circular frequency, are shown in Figures A-1 through A-24 in the Appendix.

For the vertical velocity data analysis, the

w^2-term in Equation (7) is neglected because of its second harmonic contribution. The steady velocity perturbation term $\rho W_a w$ is not a predominant term in the pressure equation for the vertical velocity case, since (according to the results of [2]) W_a is very small compared to U_a, i.e. of the order of 3-4% of U_a, at most for all conditions, except for the closest station considered (226 feet aft, full scale), where it was about 6.6% in the most severe case. This leads to a ratio of the time derivative term magnitude to this velocity term given by $\dfrac{\omega \Delta z}{W_a}$, which is about 1.7 for the lowest frequency considered in the periodic ship oscillation tests for almost all conditions, with the exception of the specific situation associated with the close-in (226 feet full scale) station. Thus the time derivative term in Equation (7) is the predominant term (for almost all the cases), but the resulting amplitude alteration and phase shift must be accounted for in the final assessment of the transfer function, expecially for the lower frequencies.

The transfer function amplitude for vertical velocity is found by converting the amplitude of the oscillatory pressure signal (from the filter output) into an equivalent "head" of water and then equating this value to that given by Equation (7), leading to

$$|w| = \frac{gH}{\sqrt{(\omega\Delta z)^2 + W_a{}^2}} \qquad (9)$$

where H is the equivalent "head" found from the calibration curves. The phase of the pressure signal, on the basis of the foregoing reasoning, would lead the actual vertical velocity by the angle

$$\tan^{-1} \frac{\omega\Delta z}{W_a} \qquad (10)$$

which must then be computed in order to correct phases measured from the recorder traces so that the proper phase of the transfer function is determined. The evaluation of the expressions in Equations (9) and (10) was quite laborious, requiring different values of W_a for each measurement point (available from [2]) and computation for each of the four frequencies of carrier pitch oscillation. The results for the vertical velocity-pitch transfer function (nondimensionalized in the same manner as the axial velocity data) are shown in Figures A-25 through A-48 in the Appendix. While the analysis technique for the vertical velocity case appears to be somewhat more questionable than that for the axial velocity, in view of the lack of a single predominant term as well as the existence of a much smaller signal level, the strong periodicity evident in the records (e.g. see Figure 20) tends to support the basic concept used herein.

Power spectrum measurements were made, for the case of no carrier motion, with the aid of a 10 volt solid state analog computer and an available wave analyzer. The wave analyzer minimum bandwidth was 7 cps, which is relatively wide for use over an entire spectral range of 40 cps (model scale), expecially in regimes of sharply varying spectra. In addition, the phase shift characteristics of the amplifiers in the analog computer, as well as the accuracy and noise level of the amplifiers (in the computer and the analyzer) relative to the input signal, had serious detrimental effects on some of the final spectral values. Since this program of power spectral measurements was introduced into the investigation as a modification and addition beyond the original program, only available instrumentation was intended to be used, and the possible defects in such spectral data must be recognized. Nevertheless, certain data (specifically the axial power spectra) are considered to have significant and useful value for the original purposes of this study, i.e. as a representation of an environmental disturbance that can be applied in simulator studies.

The power spectral density data presented in this report are defined generally for a quantity y(t), such that

$$\overline{y^2} = \int_0^\infty \Phi_y(\omega)d\omega \tag{11}$$

where $\overline{y^2}$ is the mean square value of y(t) and $\Phi_y(\omega)$ is the power spectral density. The value of the power spectral density at a particular frequency ω (rad./sec.) is defined as

$$\Phi_y(\omega) = \lim_{\substack{T\to\infty \\ \Delta\omega\to 0}} \frac{\frac{1}{T}\int_0^T y^2{}_{\Delta\omega}(\omega,t)dt}{\Delta\omega} \tag{12}$$

where $y_{\Delta\omega}(\omega,t)$ is the instantaneous amplitude of the signal at the center frequency (ω) of a filter with small bandwidth $\Delta\omega$. It is this relation, in conjunction with those of Equations (6) and (7) for identifying the velocity equivalents of the pressure signals, that was the basis of the initial power spectral density evaluations.

An illustration of the procedures used in arriving at values of the power spectra, by the methods outlined above, is given by the following description. For the axial velocity power spectra, the resultant pressure signal from the probe was sent through the wave analyzer, which was tuned to a particular frequency. The output, which is a fluctuating instantaneous amplitude of the "harmonic" component at that particular frequency, is then squared and integrated on the analog computer. This was done a number of times for each center frequency, and the average of the time averages after 40 seconds (which were all quite close) was found from the X-Y plotter curves. This value is a

mean square of the pressure signal component at frequency
ω, relative to an average value corresponding to axial
velocity U_a, and this is converted to a mean square value
of axial velocity u by use of Equation (8) and the calibration
curves. This mean square value of u is nondimensionalized
by dividing by the square of the wind-over-deck (free
stream) velocity of the tests, and the power spectral density
value of the dimensionless axial velocity perturbation is
then found by dividing this last quantity by the $\Delta\omega$ value
corresponding to the analyzer filter bandwidth. The power
spectral density is found over the desired model scale fre-
quency range by repeating this procedure for different center
frequencies. The data is converted to full scale by means
of Strouhal number scaling, i.e. maintaining the same value
of $\frac{\omega L}{U}$ for model and full scale prototype, where L is carrier
length and U is the wind-over-deck velocity (chosen as 35
knots full scale). The axial velocity power spectra obtained
in this manner are shown in Figures A-49 through A-56 in the
Appendix.

The same type of analysis was initially carried
out for the vertical velocity power spectra, but there were
two serious defects that led to the rejection of use of the
results. In the first place, the signal level of the pressure
probe output for the vertical case was very low compared to

the axial case, since it is referenced to the steady W_a value. This low signal level was therefore significantly affected by the inherent accuracy limits, noise levels, etc. of the various electronic elements used in the signal processing method described previously. The second disturbing element was the fact that the pressure signal contained contributions, at a specific frequency, from components at half that frequency because of the input from the w^2 term in Equation (7), as well as inputs that come from various "combination tones" arising from the w^2 term. (Such a problem did not exhibit itself in the case of carrier pitch motions since the predominant effect was the periodic velocity, and any possible influence of the w^2 terms, as described above, would only arise from random fluctuations that were averaged out in reading the recorder traces.) The influence of these distrubances resulted in spectral values that were much too high, especially at the lower frequencies, as determined from an evaluation of the r.m.s. vertical velocity level from the spectra, and comparison with full scale experience*.

In order to obtain some useful data on vertical

velocity power spectra, an alternate approach was developed,
which would make use of data previously recorded. (This was
done in order to avoid retesting, which would extend the
program beyond its original estimated effort.) As mentioned
earlier in the report, data was taken during the pitch
oscillation tests when there was no carrier oscillation, i.e.,
in order to provide a record of the turbulent "background"
level. The data was recorded on the Beckman recorder, after
passing through the Krohn-Hite filter, which was tuned to
the various frequencies that were used in the oscillation
tests. The pressure level recorded in this manner, for
determining vertical velocity characteristics, was a varying
signal which should essentially contain only those components
at the particular center frequency of the filter. On this
basis, the average amplitude of the almost-periodic oscil-
lations on the record was determined visually. This can be
roughly viewed as an approximation to the envelope of the
signal that is primarily at the filter frequency. Applying
the definition of Equation (12) to this data, with the
assumption that the average of the square of a signal
envelope is equivalent to $\frac{1}{2}$ (amplitude)^2, this mean square
value was then divided by the bandwidth of the filter (which
was approximately equal to $0.5\omega_c$ where ω_c is the center fre-
quency of the filter). Only four data points (at the four

pitch oscillation frequencies) were obtained in this manner, for each test position. The maximum frequency (in model scale) was 10.53 cps, hence the filter was somewhat sharper in this case than the wave analyzer filter. The resultant data was converted to a power spectral density for the vertical velocity on the basis of Equation (7), where it was assumed that the contribution of the w^2 term was neglected in carrying out this conversion of pressure data to vertical velocity data. This is certainly neglecting possible influences of the same order as those retained, but it is felt to give a good indication of the general trend of the power spectra as a function of frequency. The power spectra of vertical velocity obtained in this manner are shown in Figures A-57 through A-60 in the Appendix. The spectral levels are significantly lower than those obtained initially using the analog computer, and yield a more realistic rms vertical velocity value. It is expected that these spectral levels will be modified by Systems Technology, Inc. so that the appropriate rms values will be exhibited by the data in their simulation studies.

The difficulty of separating the velocity values to obtain a measure of spectral density from the pressure records, by use of Equation (7), is fairly evident. Another possibility for obtaining appropriate information would be

to carry out a time average of the pressure signal itself,
so that according to Equation (7) the measure of spectral
density will be obtained directly by this averaging pro-
cedure, since the terms linear in w will average out.
Nevertheless this requires feeding the data into an analog
computer, and integrating for a long period of time, so that
the same problems of noise level, accuracy, etc. present
themselves again. In view of the limits of the available
electronic analysis instrumentation, the vertical velocity
information presented herein is the best that could be
obtained under the conditions of this program.

DATA PRESENTATION AND DISCUSSION

The data obtained in this program, according to
the methods described in the previous sections, are pre-
sented in a form that may be readily approximated for use in
simulator studies. (While this data was evaluated in terms
of a wind-over-deck of 35 knots, any wind velocity can be
employed as the data is non-dimensionalized.) Appropriate
filter networks can be developed for this air wake distur-
bance data in a manner similar to that outlined in [1].
Since that task is the province of Systems Technology, Inc.,
or others who may utilize such information, no further

discussion of the methods of wake disturbance simulation will be given here. However, a few general comments on trends indicated by the data presented as graphs in the Appendix will be made.

Data for Horizontal Velocity Fluctuations Associated With Carrier Pitch Motion

The pitch transfer function amplitudes are presented in Figures A-1 through A-8 for the wind condition of 3° port. In general, the value of the function decreases as the distance aft of touchdown increases. For example, the magnitude of the function 1040 feet aft of touchdown is about 10% of the value 226 feet aft of touchdown (condition 47 feet port of glide path centerline). Also, the positions port of the glide path centerline tend to have amplitudes of greater magnitude than either the center-line or starboard positions. Here, for example, (and again at the position 226 feet aft of touchdown) the 47 feet port position has a maximum value slightly more than three times that existing at the 47 feet starboard position. While the angle of the glide path also affects the value of the function, trends are not so definitive.

The data for the condition of wind 10° port is shown in Figures A-9 through A-16. As in the case of wind 3° port, the magnitude of the pitch transfer function

amplitude decreases as the distance aft of touchdown increases, but the amount of decrease is only about 50%. The value of the amplitude also tends to be somewhat higher; thus at 1040 feet aft of touchdown the maximum value of the amplitude is about five times that existing with the wind 3° port. The trend of decreasing values as the position in space is moved from port to starboard locations is again repeated.

The horizontal velocity fluctuations-pitch transfer function phase data for the condition of wind 3° port are shown in Figures A-17 through A-20, while that for the condition of wind 10° port are shown in Figures A-21 through A-24. In general, the slope of the phase angle as a function of frequency increases as the distance aft of touchdown increases. The direction of the wind, i.e. whether 3° or 10° port, and the position in space about the glide path, i.e. port or starboard, does not significantly affect the slope of the function as plotted with increasing ω values.

Data for Vertical Velocity Fluctuations Associated with Carrier Pitch Motion

The pitch transfer function amplitudes are presented in Figures A-25 through A-40. These amplitude values were higher by a factor of about 2 just aft of the carrier to as high as a factor of 5 at the farthest downstream position

when compared with amplitudes associated with horizontal velocities.

While the amplitudes were somewhat higher for the condition of wind 10° port compared with the wind 3° port, the difference was not as large as for the case of horizontal velocity fluctuations. In fact, at ?:⁻ ⁻ : :ft of touch-down, the condition of wind 3° port resulted in somewhat higher values than with the wind 10° port. The amplitude decreased as the distance aft of touchdown increased with the condition of wind 3° port having a greater decrease than the condition of wind 10° port. The variation in amplitude from port to starboard positions about the glide path also existed. No one glide path was optimum for the entire approach distance examined.

The vertical velocity fluctuation-pitch transfer function phase data is presented in Figures A-41 through A-48. In general, the same conclusions can be drawn from the data as from the data obtained with horizontal velocity fluctuations. The wind direction (?° or 10° port), the position in space (centerline, port or starboard of center-line), or the glide path angle has little effect on the slope of the phase curves with respect to frequency. The slopes did tend to increase as the distance aft of touchdown in-creased.

Power Spectra Data - Horizontal Velocity Fluctuations

This data is presented in Figures A-49 through A-56. The general trend, as would be expected, is a rather rapid decrease in the power spectral magnitude with increasing ω values. With the wind 10° port, the spectral amplitude is greater than with the wind 3° port. The magnitude also decreases with an increase in distance aft of touchdown.

There are two curves in this series of graphs about which a few additional comments will be made. The first one is Figure A-50., which presents data for the condition of wind 3° port 485 feet aft of touchdown. Here there is a "peak" in what would normally be a continuously decreasing function. The peak occurs at a full scale ω value of about 2. One possible cause for this seemingly erratic behavior of the data is the fact that this position in space is that area where the disturbed flow from the island and that from the disk edges join, as observed during the flow visualization studies [2].

The other curve is that shown on Figure A-53 which is for the condition of wind 10° port 226 feet aft of touchdown. In this case, the magnitude of the function appears lower than what seems reasonable in view of tne data obtained at positions further aft of touchdown. No

explanation can be offered for this apparent inconsistency.

Power Spectra Data - Vertical Velocity Fluctuations

This data is presented in Figures A-57 through
A-60. As pointed out in the section on Data Evaluation,
this data was obtained from Beckman recorder traces of the
probe output without model motion using a technique
similar to that used when there was model motion. This
data also illustrates a rapid magnitude decrease with an
increase in ω value, as anticipated. The condition of
wind 10° port produces magnitudes greater than those
associated with wind 3° port.

SUMMARY AND CONCLUSIONS

This experimental study permits conclusions
to be drawn in the general areas of instrumentation and test
data. From the test data, certain applications to the landing
problem itself can be hypothesized.

Instrumentation

A probe used to sense fluctuating horizontal and
vertical velocities (in water) was successfully developed.
The design of the unit is based on a Prandtl type pitot with
the total and static pressures fed to separate transducers.
The response of the transducers is matched, thus subtracting

one electrical signal from the other leaves a measure of the velocity head. The probe response under dynamic calibration is good to about 40 cps. The basic design may be satisfactory for higher frequencies, but unwanted "side effects" in the dynamic calibration techniques employed here are believed to affect the accuracy of the calibration at higher frequencies. The frequency range achieved was more than adequate for the purpose of this investigation.

Test Data

The general conclusions drawn from this series of studies reinforces those deduced from earlier flow visualization and "steady" flow investigations [2].

Functions Associated with Horizontal Velocity Fluctuations

1. The magnitudes of the pitch transfer function amplitude are larger for the condition of wind 10° port than with the wind 3° port.

2. The magnitudes of the pitch transfer function amplitude decrease with downstream distance aft of touchdown for both conditions of wind 3° and 10° port.

3. The rate of decrease (with distance) of the pitch transfer function amplitude is greater for the condition of wind 3° port than with the wind 10° port.

4. The magnitude of the pitch transfer function de-
    creases as the position in space moves from port
    to starboard of the glide path centerline.

5. The slope of the pitch transfer function phase
    with frequency tends to increase with an increase
    in distance aft of touchdown. Wind direction, glide
    path angle, and position in space (i.e. on the
    glide path centerline or port or starboard of the
    centerline) has little effect on the phase value.

Functions Associated with Vertical Velocity Fluctuations

6. The magnitudes of the pitch transfer function
    amplitude are larger (by factors up to 5) when com-
    pared with magnitudes associated with horizontal
    velocity fluctuations.

7. The magnitudes of the pitch transfer function
    amplitude decrease with increasing distance aft of
    touchdown for both conditions of wind 3° port and
    10° port.

8. In general, the amplitudes of the pitch transfer
    function are larger for the condition of wind 10°
    port than with wind 3° port.

9. With the wind 10° port, the rate of decrease in
    the pitch transfer function amplitude is less than
    with the wind 3° port.

10. The amplitude of the pitch transfer function decreases as the position in space moves from port to starboard of the glide path centerline.

11. The slope of the pitch transfer function phase with frequency tends to increase with an increase in distance aft of touchdown. Wind direction, glide path angle, and position in space (i.e. on the glide path centerline or port or starboard of the centerline) has little effect on the phase value.

Power Spectra

12. The magnitude of the power spectra curves decreases with increasing ω, as expected.

13. For the condition of the wind 3° port, the magnitude of the spectra for both horizontal and vertical velocity fluctuations are about the same when within 500 feet aft of touchdown. For distances further aft, the magnitudes of the vertical velocity power spectra remain larger.

14. For the condition of wind 10° port, the vertical velocity fluctuations produce power spectra values about ten times that of the horizontal velocity fluctuations.

(These comments are based upon an analysis technique for the vertical velocity case that does not have the same expected degree of validity as for the horizontal velocity case.)

Interpretation of Data in Relation to Aircraft Operations

The significance of this data in terms of influencing aircraft operations can be determined only through simulator studies, as the investigations reported here only present the velocity fluctuations and power spectra associated with the velocity field encountered by the aircraft. These studies cannot indicate how the aircraft will respond to such flow variations. However, the data can be summarized in the form of several major conclusions which are related to the landing operation. These conclusions are only valid if simulator studies show that the disturbances (as reported here) significantly influence the flight characteristics of the aircraft during a carrier landing approach.

1. Concerning pitch transfer function amplitude associated with both the horizontal and vertical velocity fluctuations, it appears that shifting the wind-over-deck direction from along the centerline of the landing deck towards the keel of the ship would offer benefits. This alteration should only be considered if satisfactory landing characteristics of the aircraft can still be maintained, in spite of the additional strain on the landing gear because of the cross-wind landing approach.

The suggested change in wind-over-deck direction is made
because the magnitude of the pitch transfer function
amplitude decreases as the wind direction shifts towards
the keel-line of the ship.

Regardless of the wind-over-deck direction, the
pilot should attempt to avoid drifting port of the center-
line of the glide path, as the magnitude of the pitch
transfer function amplitude increases as the position
in space moves port of the glide path centerline. (For
example, a change of the position in space from 47 feet
starboard of the glide path to 47 feet port of the glide
path increases the magnitude of this function by a factor
of 3.)

2. Concerning the pitch transfer function phase associated
    with both the horizontal and vertical velocity fluctuations,
    there is no one wind orientation or aircraft orientation
    which produces a condition noticeably improved over any
    other condition tested. Therefore, any operational modi-
    fication should only be directed toward altering the
    effect of the transfer function amplitude.

3. From power spectra considerations, for both horizontal
    and vertical velocity fluctuations, the wind-over-deck
    direction again should be changed from the centerline of
    the landing deck towards the ship's keel-line if such a

shift is possible without increasing other landing hazards.
While the glide path angle does have an effect, no one
glide path angle is superior during the entire approach.

It is recognized that introducing the changes mentioned
above would reduce the intensity of the time-varying wake distur-
bances encountered during a landing approach. However, consider-
ation must be made of the difficulties of cross-wind landings
and the additional hazard to the pilot and the aircraft during a
cross wind landing. Simulator studies as undertaken by Systems
Technology, Inc., should provide an estimate of the benefits
which might accrue by incorporating the suggestions mentioned
above, and these potential benefits could then be weighed against
the additional hazards or difficulties introduced in an attempt
to achieve these benefits. A possible long-range objective,
which should be investigated further, would incorporate a re-
duction of the landing deck cant angle, thus gaining the benefits
of a reduction in the glide path disturbances while also reducing
the necessity of a cross-wind landing approach.

There does not appear to be an optimum glide path
angle which would reduce the effect of air-wake disturbances
for all possible conditions studied during this investigation.
Therefore, no particular glide path angle can be recommended
from the information gained during these studies.

REFERENCES

1. Durand, T. S. and Teper, G.L.: "An Analysis of Terminal Flight Path Control in Carrier Landing," Systems Technology, Inc., Report No. 137-1, August 1964

2. Lehman, A. F.: "An Experimental Study of the Dynamic and Steady State Flow Disturbances Encountered by Aircraft During a Carrier Landing Approach," Oceanics, Inc., Report No. 64-16, September 1964.

3. Hubbard, P. G.: "Operating Manual for the IIHR Hot-Wire and Hot-Film Anemometers," State University of Iowa Studies in Engineering, Bulletin, 37, 1957.

    Ling, S. C.: "Measurement of Flow Characteristics by the Hot-Film Technique," State University of Iowa, Ph.D. Thesis, 1955.

4. Ippen, A.T.,Tankin, R.S. and Raichlen, F.: "Turbulence Measurements in Free Surface Flow with an Impact Tube-Pressure Transducer Combination," Massachusetts Institute of Technology, Report No. 20, July 1955.

5. Corcos, G. M.: "Pressure Measurements in Unsteady Flows," Symposium on Measurement in Unsteady Flow, ASME Hydraulic Division Conference, May 21-23 1962.

APPENDIX

GRAPHS OF EXPERIMENTAL DATA

See Part II